Powder X-ray and neutron diffraction

Lecture series: Modern Methods in Heterogeneous Catalysis Research

Malte Behrens, FHI-AC
behrens@fhi-berlin.mpg.de

With Figures taken from different sources: See last slide

Outline

- Fundamentals of XRD
- Experimental aspects
- Phase identification
- Phase characterization: Ideal structure
- Phase characterization: Real structure
- Neutron diffraction

With examples from heterogeneous catalysis

XRD Overview

- X-ray scattering techniques are among of the most widely applied methods used for the characterization of solids
- 1895: Discovery of X-rays (W.C. Röntgen)
- 1912-13: Pioneering experiments by W. Friedrich, P. Knipping and M. von Laue and W.H. and W.L. Bragg
- 1921: Full interpretation by P.P. Ewald
- Since 1950: XRD has become a standard laboratory technique
- 1967: Full pattern refinement by H.M. Rietveld
- Since 1980: New technical opportunities with the easy access to synchrotron radiation
- Current trends in catalysis research: XRD under reactive conditions, combination with other complementary techniques, and development of evaluation methods for a detailed defect analysis

Fundamentals of diffraction

- Transverse plane waves from different sources can “interfere” when their paths overlap
- constructive interference (in phase)
- destructive interference (out of phase), completely destructive for the same amplitude and wavelength
- partially destructive for different amplitudes and wavelengths

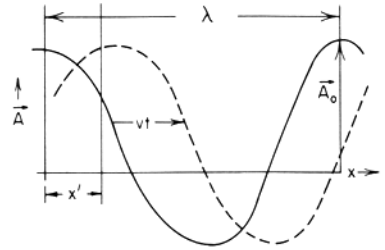

FIG. 3-1. A cosine wave moving to the right.

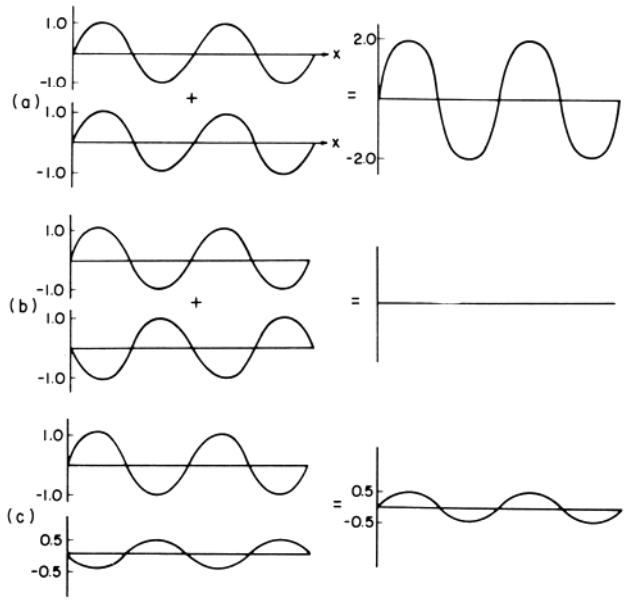

FIG. 3-2. Interference between two waves. Both waves are assumed to have the same maximum amplitude (unity) except in (c) and the same wavelength in all cases. (a) Constructive interference; (b) complete destructive interference; (c) partial destructive interference.

Diffraction experiments

- Interference patterns can be produced at diffraction gratings (regularly spaced “slits”) for $d \approx \lambda$
- Waves from two adjacent elements (1) and (2) arrive at (3) in phase if their path difference is an integral number of wavelengths
- Kinematic theory of diffraction:
  - R >> d: contributions of each beam can be taken as a plane traveling wave
  - Conservation of energy in the scattering process
  - A once-scattered beam does not re-scatter
- Periodically arranged atoms (crystals) act as diffractions gratings for radiation $0.6 \leq \lambda \leq 1.9$ Å

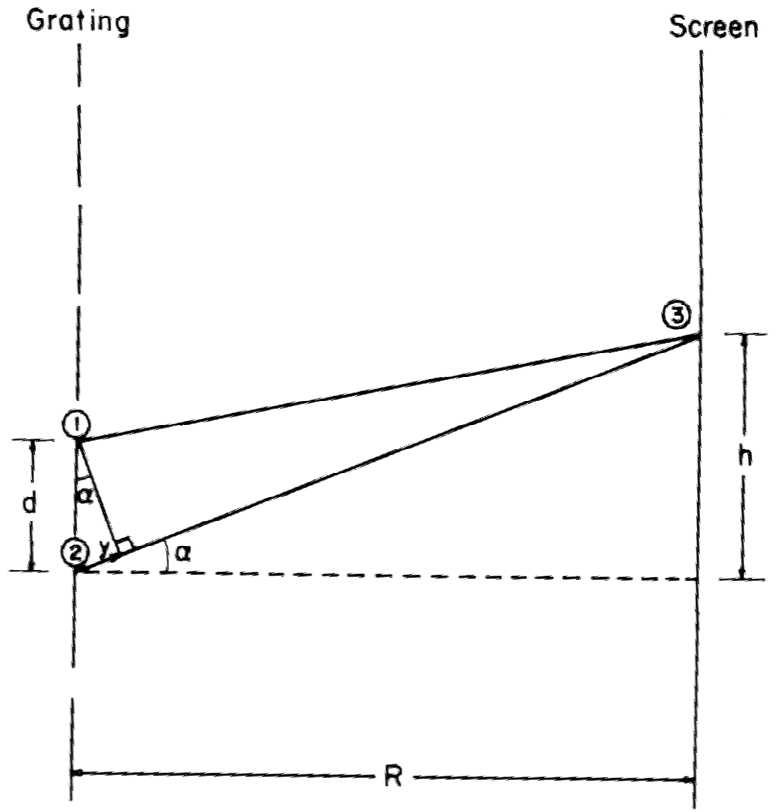

The Bragg equation

- GE = EH = d sinθ
- nλ = 2d sinθ (Sir W.L. Bragg)
  - 2d < λ: no diffraction
  - 2d > λ: different orders of diffractions (n= 1, 2, …) at different angles
  - 2d >> λ: 1st order reflection too close to direct beam

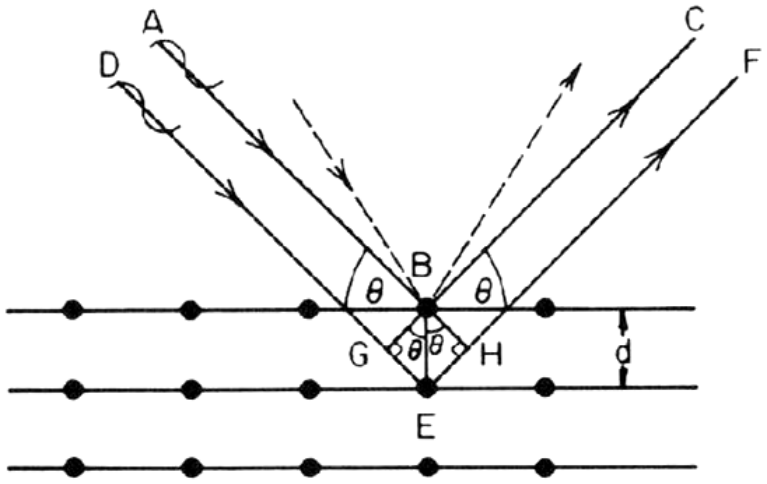

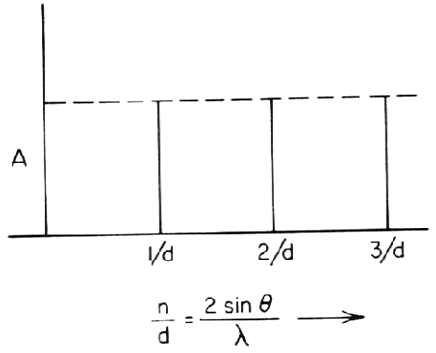

FIG. 3-5. Amplitude versus 2 sin θ/λ.

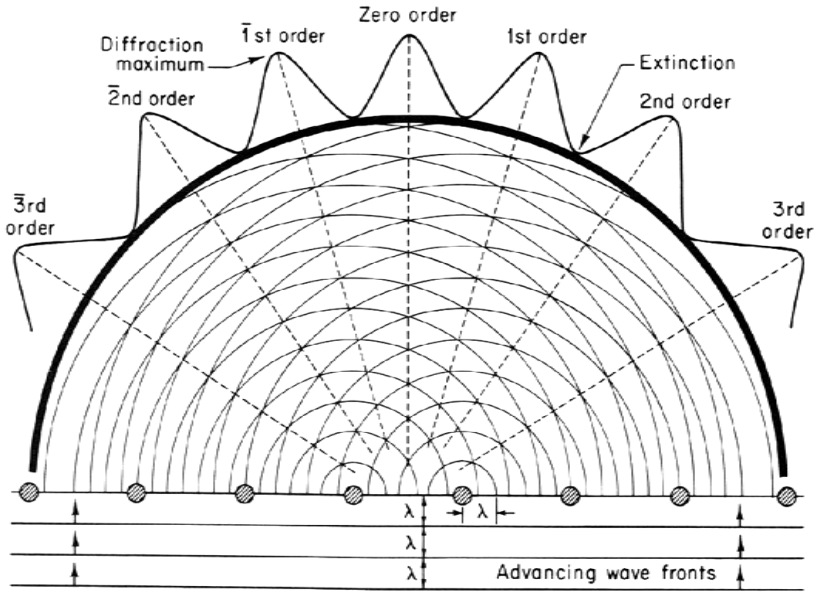

Fig. 3-1. Reinforced scattering by a regularly spaced row of atoms.

Towards diffraction patterns

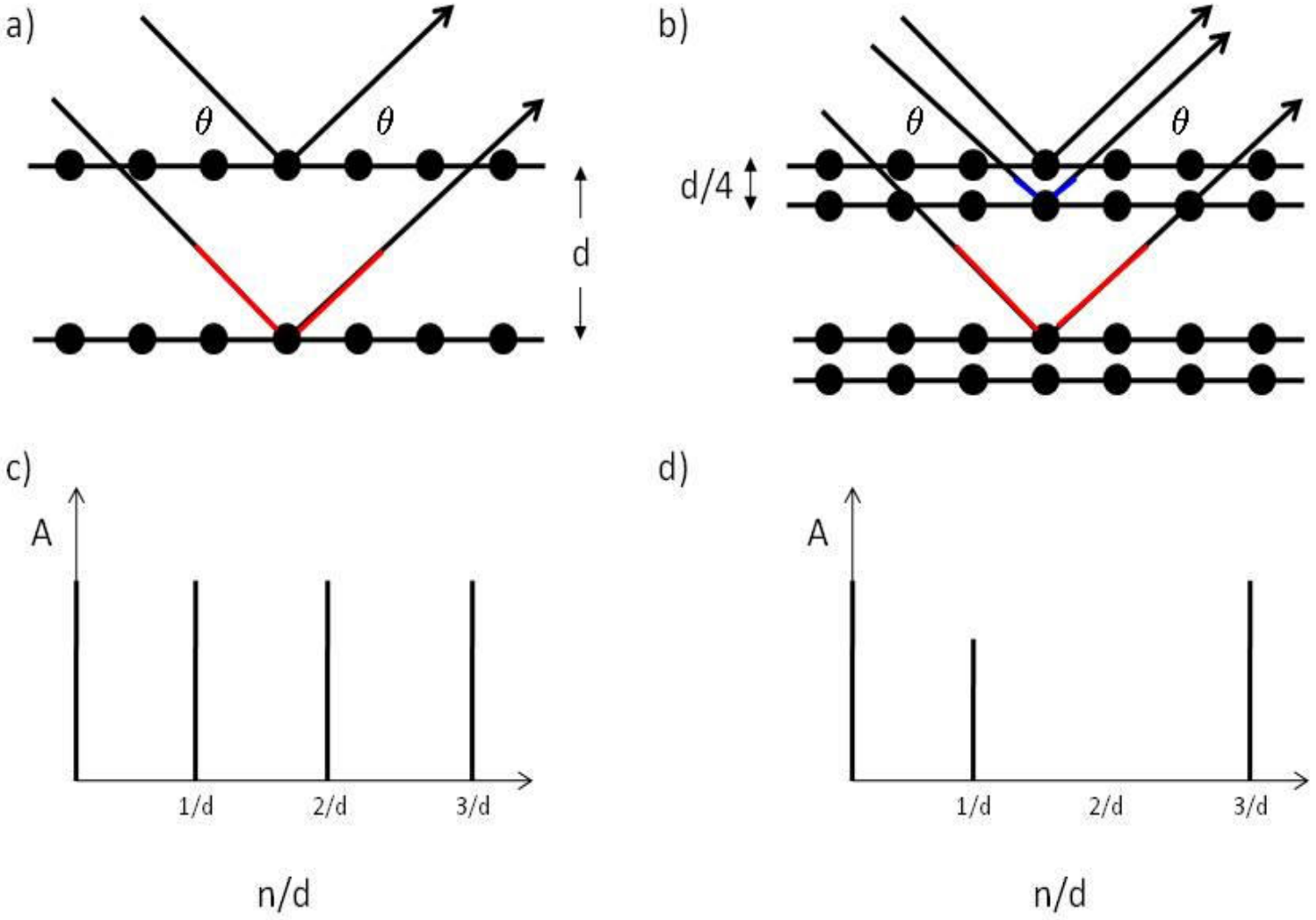

Crystal lattices as gratings

- Crystals can be described as three-dimensional lattices
- A lattice point at the origin of the unit cell is reproduced by three translations *a*, *b* and *c* and three angles α, β and γ, (lattice or unit cell parameters)
- An infinite number of lattice planes run through the lattice points and their orientation with respect to the unit cell is given by the fractional parts of the cell axes at which they intercept
- Sets of equally spaced and parallel lattice planes are defined by Miller indices *hkl*, representing the reciprocals of these intercepts in the directions of *a*, *b* and *c*.
- The spacing of adjacent planes is termed d_{hkl} and, for example, in a cubic lattice $d_{100} = d_{010} = d_{001} = a$ and $d_{200} = d_{020} = d_{002} = a/2$.

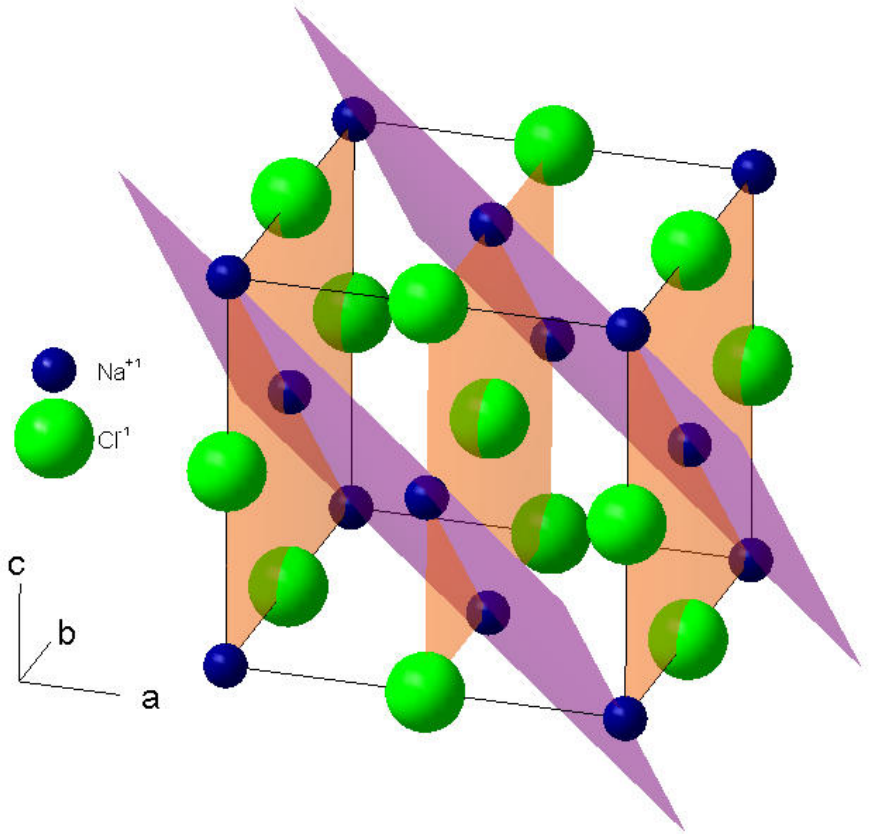

A simple crystal structure

- Cubic lattices: $a = b = c$; $\alpha = \beta = \gamma = 90°$
- Other lattice symmetries: hexagonal, trigonal, tetragonal, orthorhombic, monoclinic and triclinic
- A crystal structure: lattice parameters + coordinates *x*, *y* and *z* as fractions of *a*, *b* and *c* of crystallographically independent atoms (asymmetric unit), + space group (symmetry operations needed to reproduce the asymmetric unit to completely fill the unit cell)
- NaCl: cubic, *a* = 5.6402 Å, Na: *x* = 0, *y* = 0 and *z* =0, Cl = *x* = ½, *y* = ½ and *z* = ½, *F*m-3m

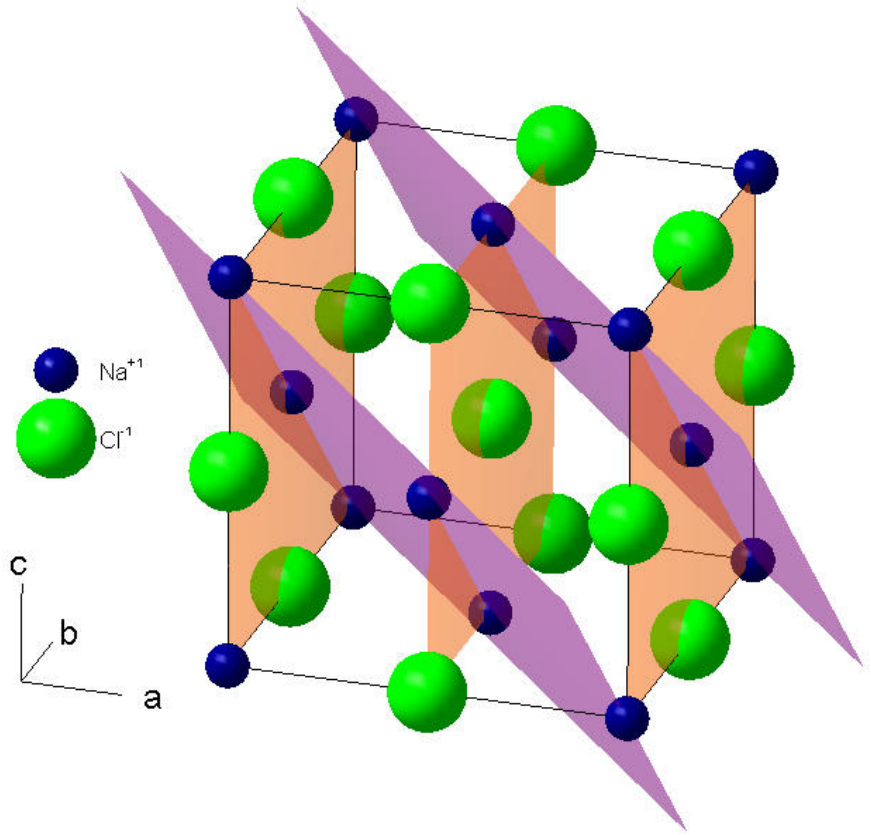

Powder method

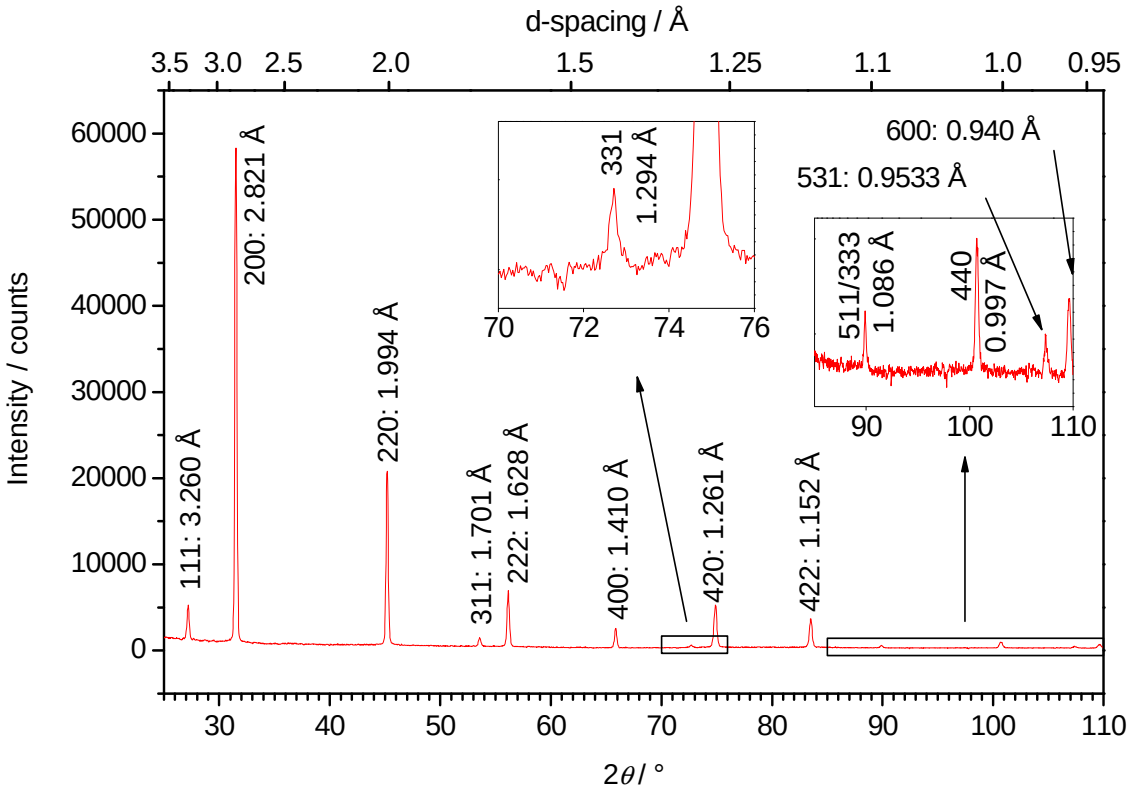

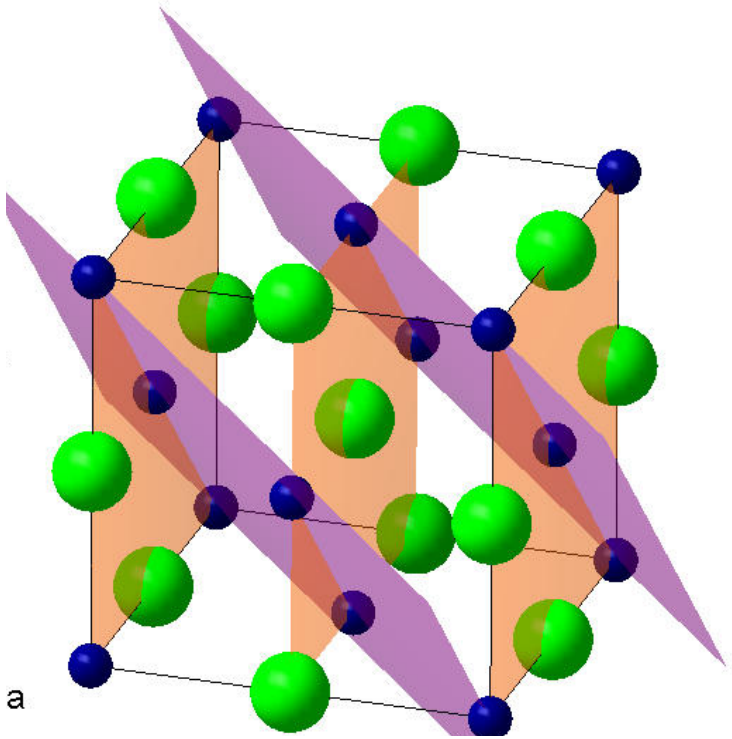

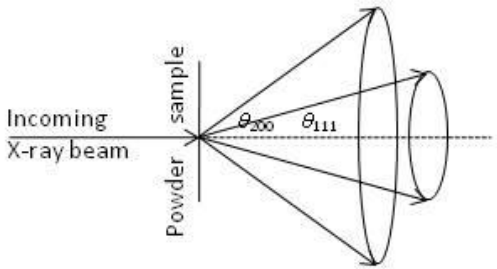

Scattered intensity and crystal structure

- Total scattering power of a reflection

$$P = I_0 \frac{V \cdot \lambda^3 \cdot m \cdot F^2}{4 \cdot v_a^2} \left(\frac{1 + \cos^2 2\theta}{2 \cdot \sin \theta} \right) \left(\frac{e^4}{m_e^2 c^4} \right)$$

  - m: multiplicity, v_a: volume of unit cell, V: illuminated volume of powder sample

- The structure factor F_{hkl}
  - $I_{hkl} \sim |F_{hkl}|^2$
  - $F_{hkl} = \Sigma f_{jT} \exp 2\pi i(h \cdot x_j + k \cdot y_j + l \cdot z_j)$
  - f_{iT}: atomic scattering factor

Atomic scattering factor

- X-ray photons interact with the electron clouds of an atom
- electron clouds are not points in space, but possess a finite size of the same magnitude as the X-ray wavelength
- electrons are spread in space and consequently not all are scattering in phase, the scattering amplitude will vary with 2θ
- atomic scattering factor (ratio of the amplitude scattered by an atom to that scattered by a single electron) fall off with $(\sin\theta)/\lambda$
- As a consequence, the Bragg peaks at higher angles will generally exhibit a lower intensity compared to those at lower angels

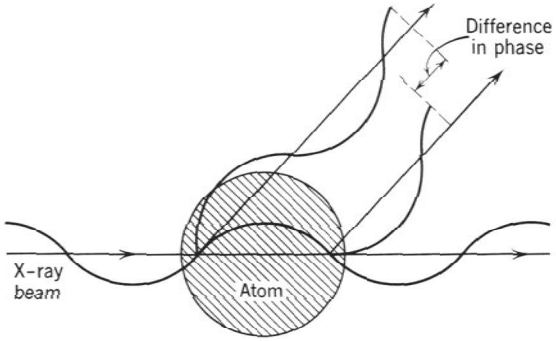

Fig. 3-14. *Phase difference in scattering from* different parts of an atom.

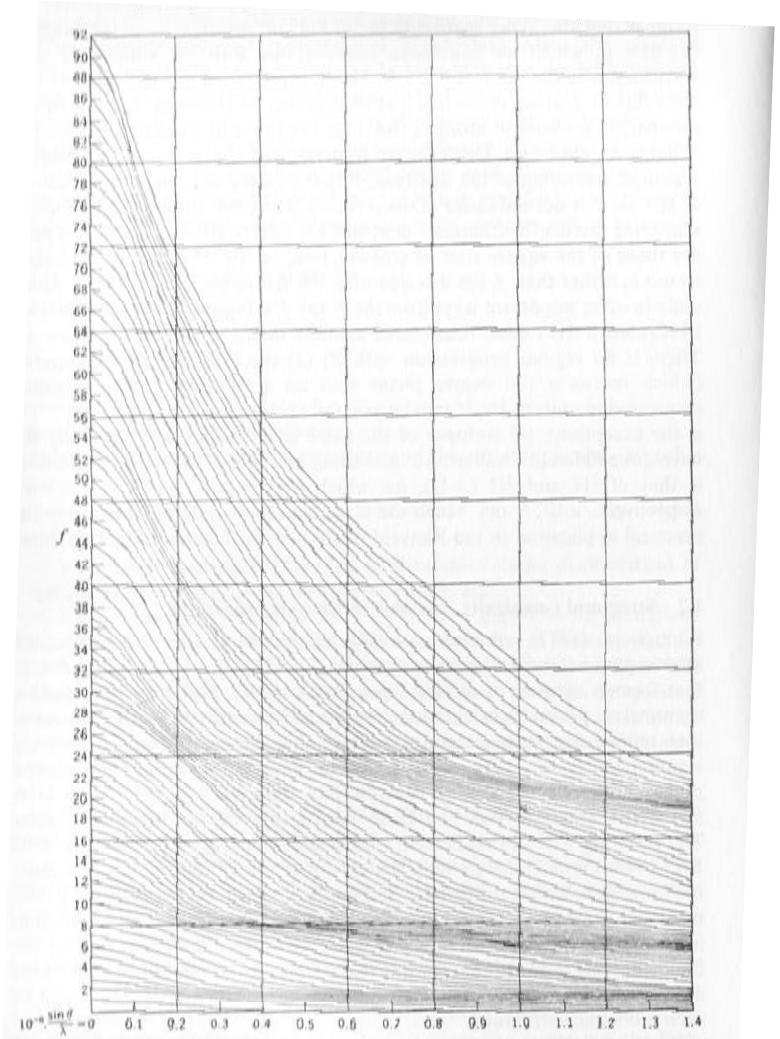

Fig. 1.2 The X-ray atomic scattering factor, f, shown as a function of $(\sin\theta)/\lambda$ for neutral atoms. The numbers along the ordinate are the atomic numbers, Z. (From Buerger 1942.)

Information content of an XRD pattern

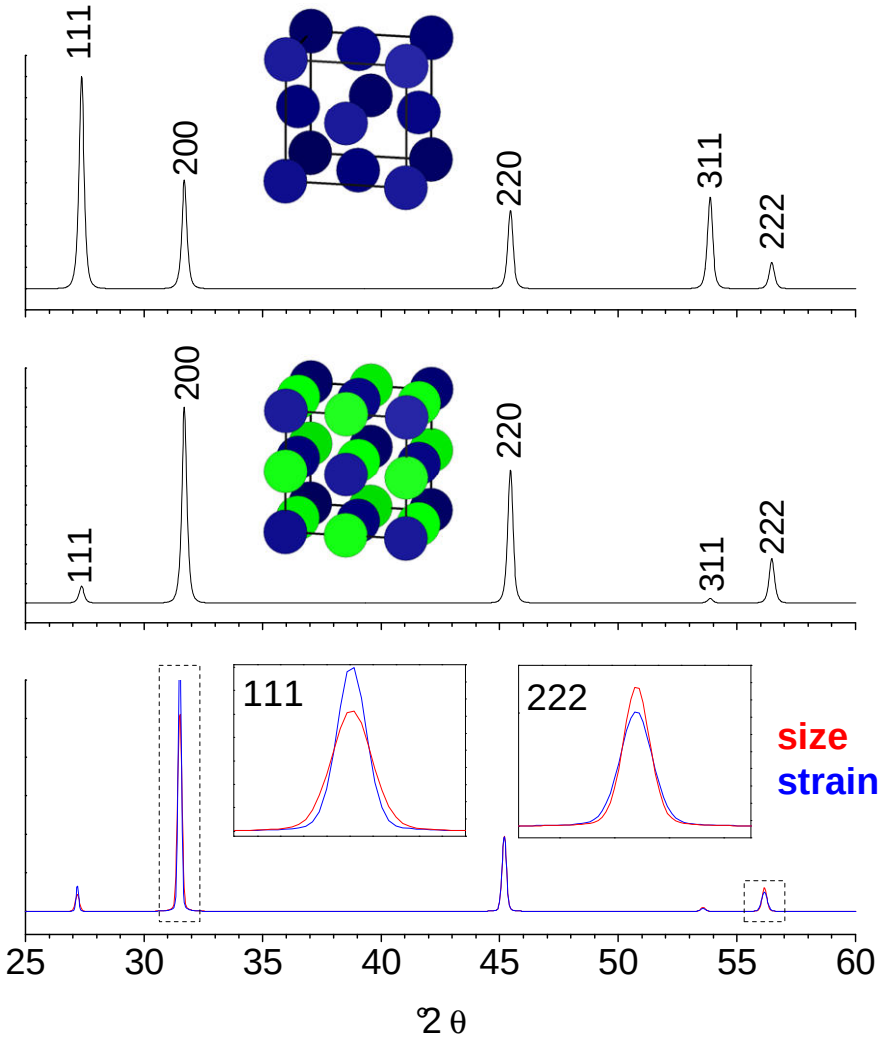

What can we learn from a diffraction experiment?

- Are there peaks? (Crystallinity)
- Which crystalline phases are present? (Phase identification, database of fingerprint patterns)
- How many crystalline phases are present? (Homogeneity)
- Relative amount of phases? (Quantitative phase analysis)
- Crystal structure refinement (ideal structure)
- Size, strain, defects (real structure)

Experimental: X-rays

- X-ray have wavelengths around 1 Å (≈ d) (W.C. Röntgen, 1895)
- Easily produced in X-ray tube

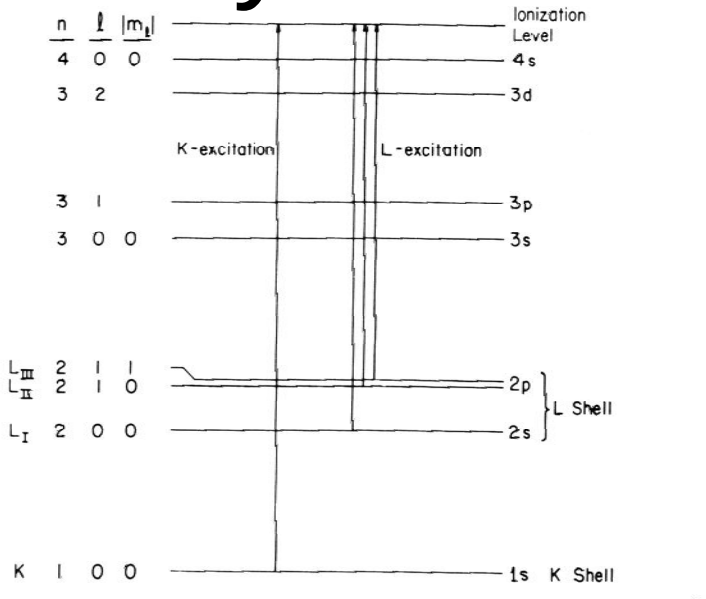

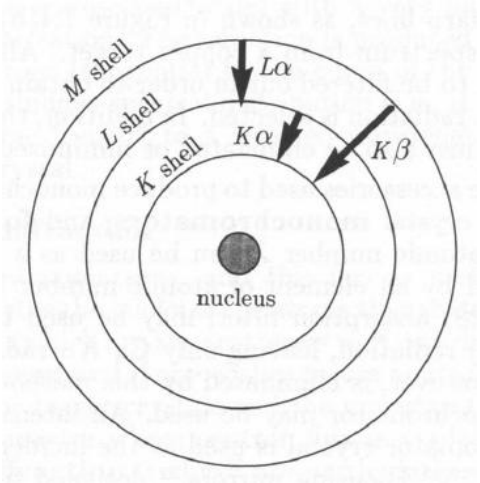

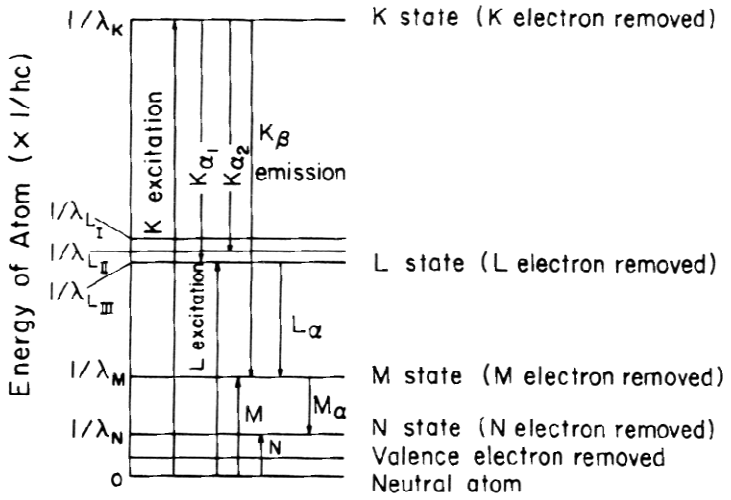

X-ray tubes

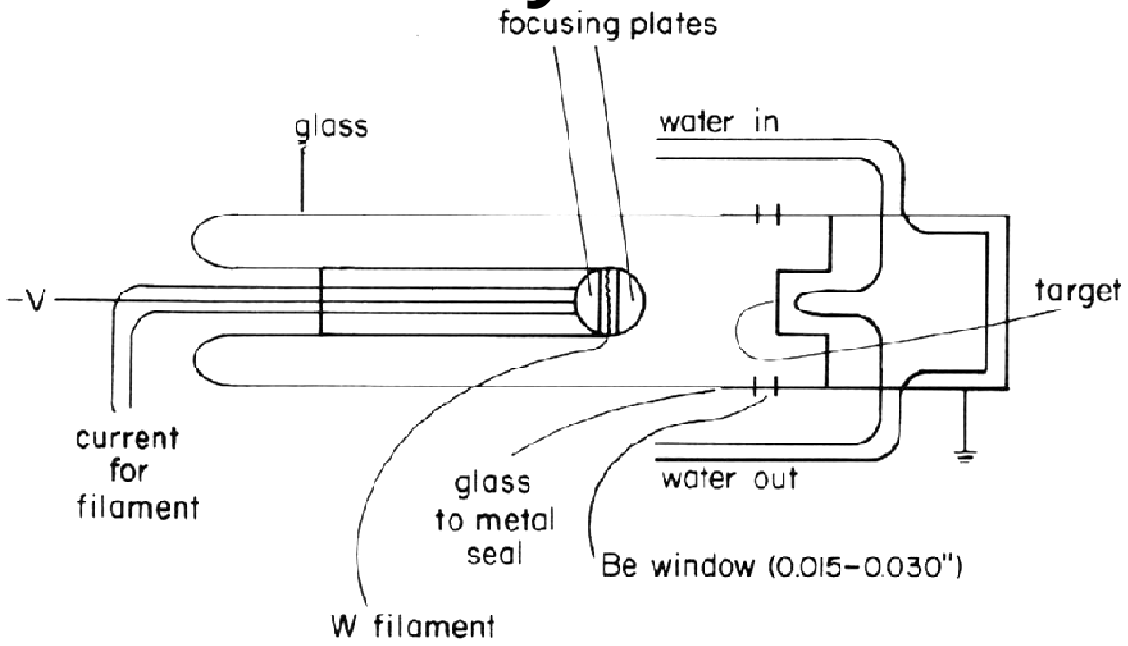
focusing plates
glass
water in
-V
target
current
for
filament
glass
to metal
seal
water out
Be window (0.015–0.030")
W filament

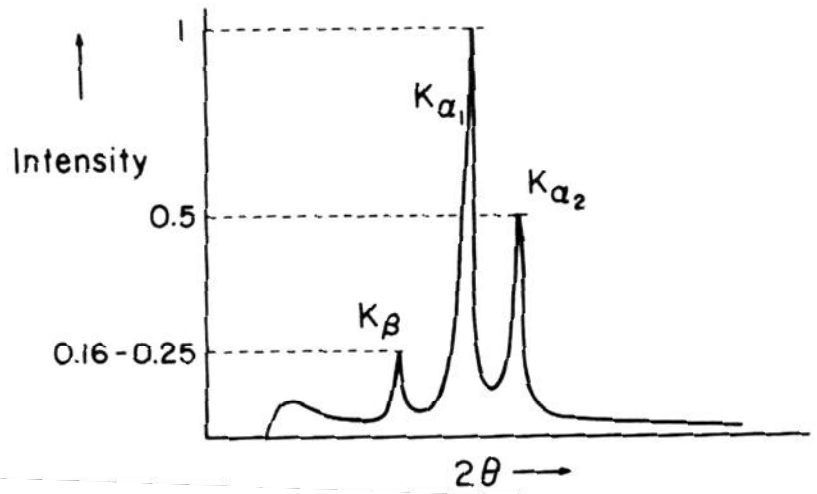
I
Intensity
0.5
0.16 - 0.25
K_{α_1}
K_{α_2}
K_β
2θ

Geometry of diffractometers

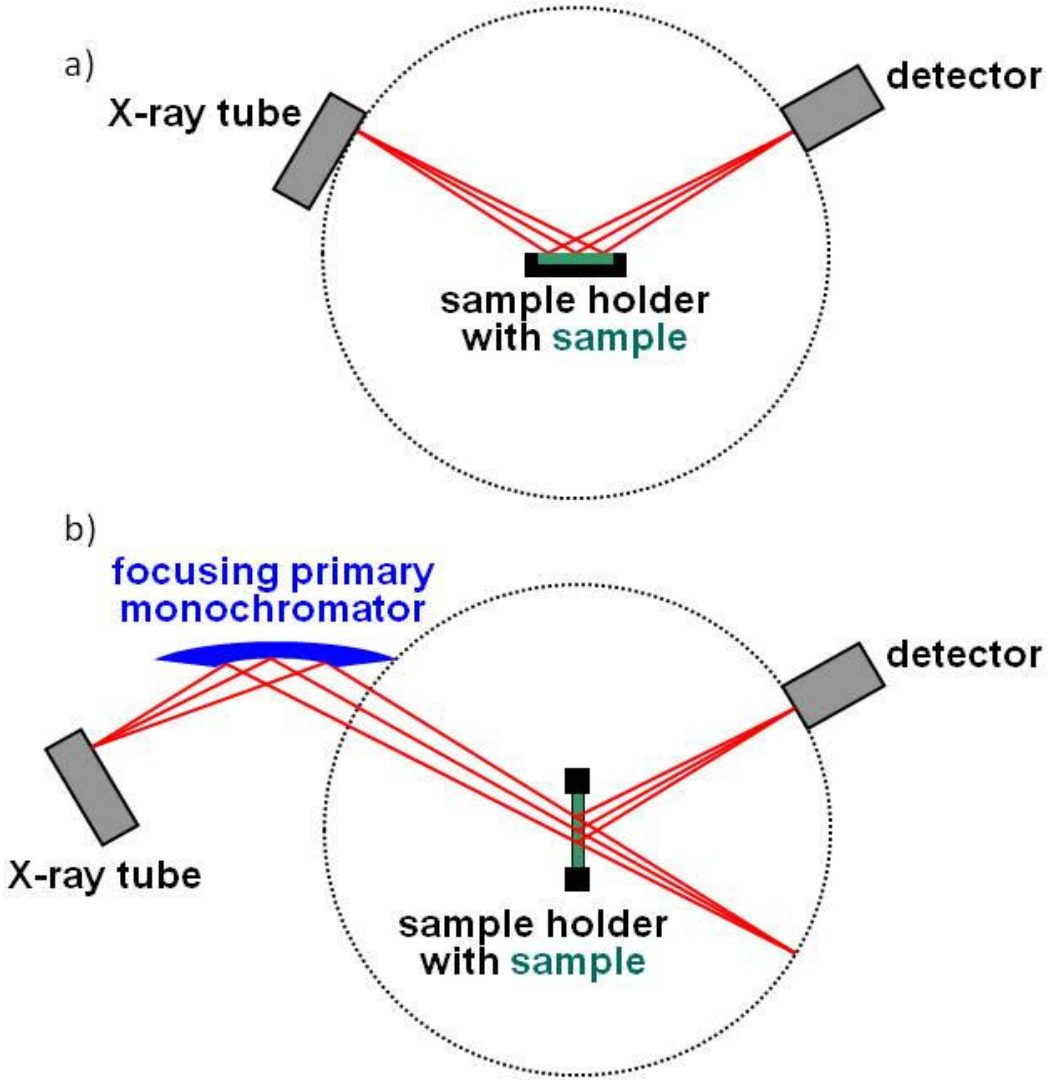

- Reflection geometry
  - θ-2θ
  - θ-θ
- Transmission geometry

Phase analysis

- Peak positions and intensities are compared to a patterns from the powder diffraction file (PDF) database
- Generally, ALL peaks found in a PDF pattern must also be seen in in the diffractogram, otherwise it is not a valid match
- Possible exceptions:
  - Small peaks may be not detectable if the noise level is too high
  - Missing peaks may be the result of a very strong preferred orientation effect (intensities systematically hkl-dependent)
  - “Missing” peaks may be the result of anisotropic disorder (FWHMs systematically hkl-dependent)
  - Very small residual peaks may be artifacts resulting from spectral impurities (other wavelengths, e.g. Kβ, W L)
  - The peaks are real, but they belong to the reference compound, not an impurity. It may be that your diffraction pattern is “better” in terms of signal/noise ratio than the (possibly old) PDF pattern. After all, the diffractometers have improved with time (Rietveld check required)
- Systematic shifts of peak position might be due to thermal expansion (check PDF entry) or different composition

F.Girgsdies

Phase identification: PDF database

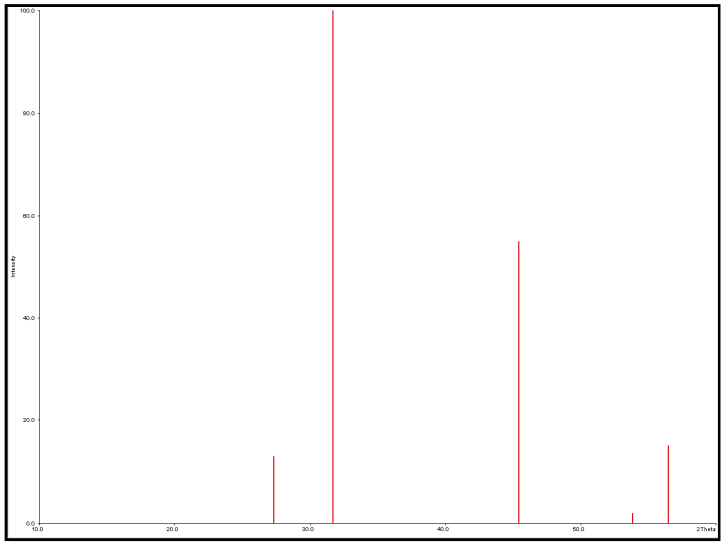

d[A]	2Theta	Int.	h k l	d[A]	2Theta	Int.	h k l
3.2600	27.335	13	1 1 1	0.9969	101.193	2	4 4 0
2.8210	31.693	100	2 0 0	0.9533	107.809	1	5 3 1
1.9940	45.450	55	2 2 0	0.9401	110.046	3	6 0 0
1.7010	53.853	2	3 1 1	0.8917	119.504	4	6 2 0
1.6280	56.479	15	2 2 2	0.8601	127.169	1	5 3 3
1.4100	66.229	6	4 0 0	0.8503	129.893	3	6 2 2
1.2940	73.066	1	3 3 1	0.8141	142.240	2	4 4 4
1.2610	75.304	11	4 2 0				
1.1515	83.973	7	4 2 2				
1.0855	90.409	1	5 1 1				

[5-628] PDF-2 Sets 1-81 Quality: * Wavelength: 1.540598

Sodium Chloride
Halite, syn
Na Cl

Rad.: CuKa1 (1.5405) Filter: Beta Ni d-sp:
I/Icor.:4.40 Cutoff: Int.: Diffractometer
Ref.: Swanson, Fuyat., Natl. Bur. Stand. (U.S.), Circ. 539, II, (1953), 41

Sys.: Cubic S.G.: Fm-3m (225) V(redu): 44.8
a: 5.6402 b: c:
A: B: C: Z: 4 mp: 804deg
Dx: 2.164 Dm: 2.168 SS/FOM: F17= 92.7 (.0108, 17)

---

ea: nwB: 1.542 ey: Sign: 2V:
Color: Colorless
Ref.: Dana's System of Mineralogy, 7th Ed., II, 4

An ACS reagent grade sample recrystallized twice from hydrochloric // acid. // Pattern taken at 26 C. // See ICSD 18189 (PDF 72-1668).

Phase identification: Examples

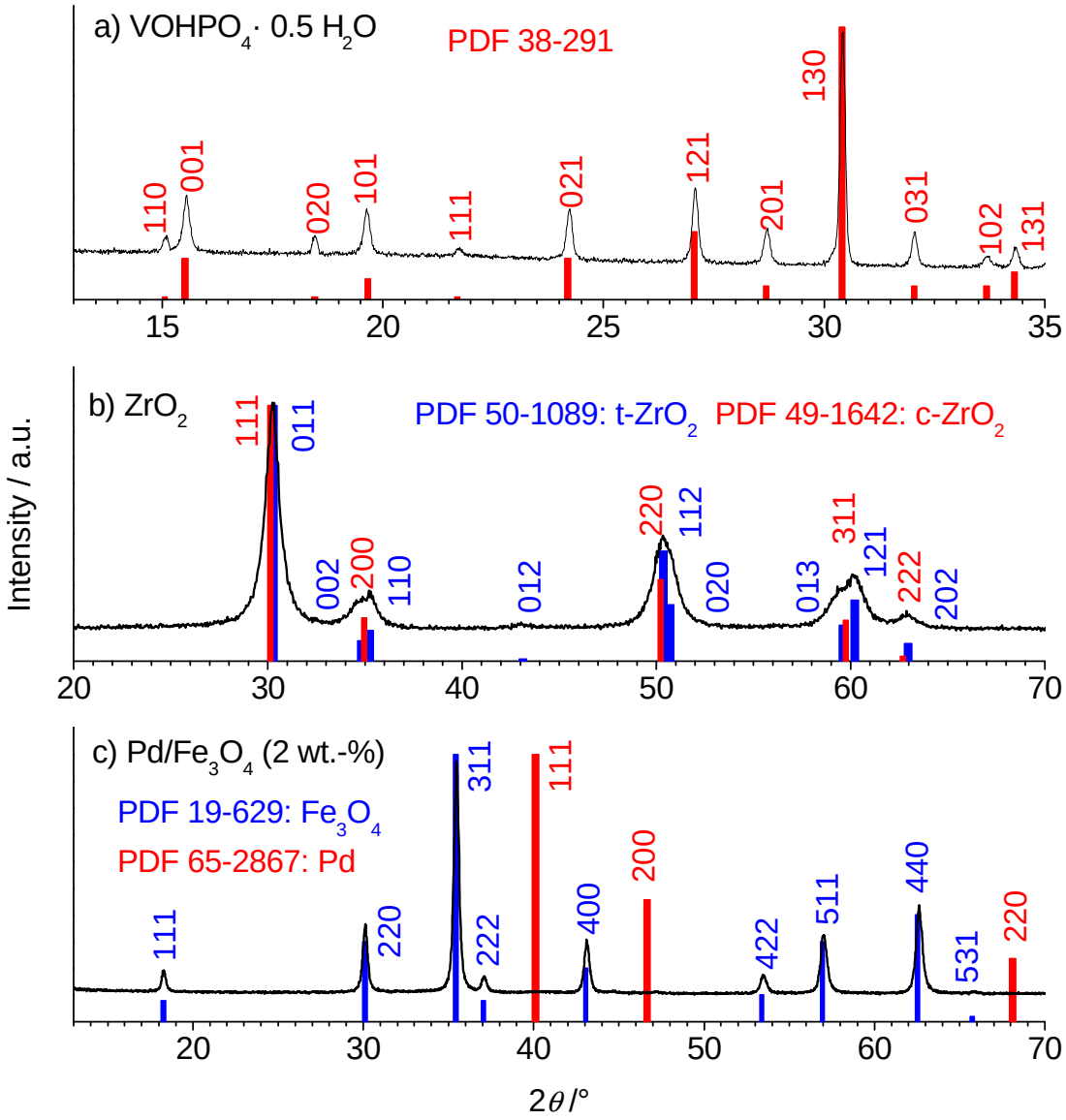

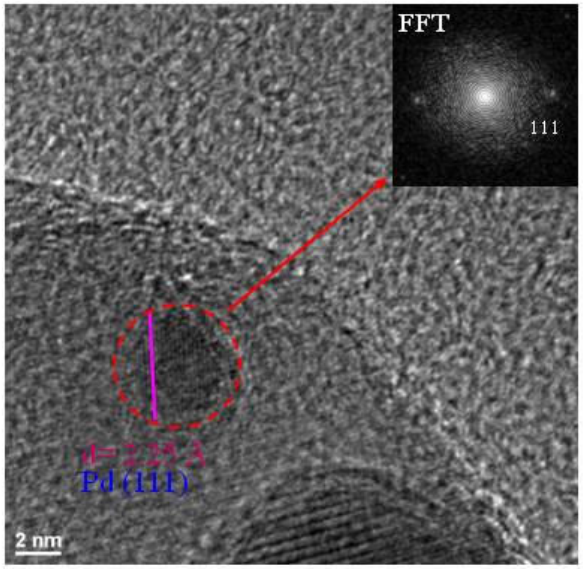

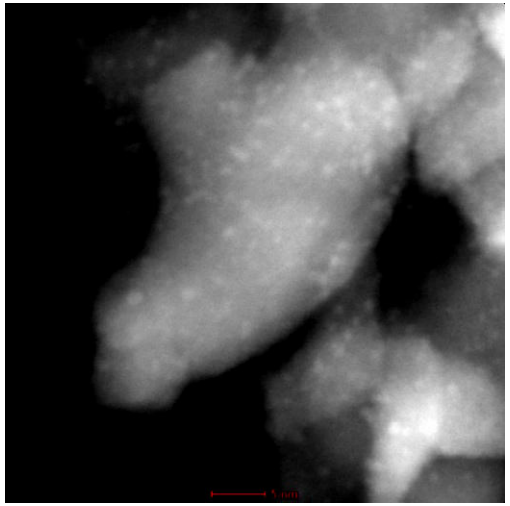

Phase mixtures

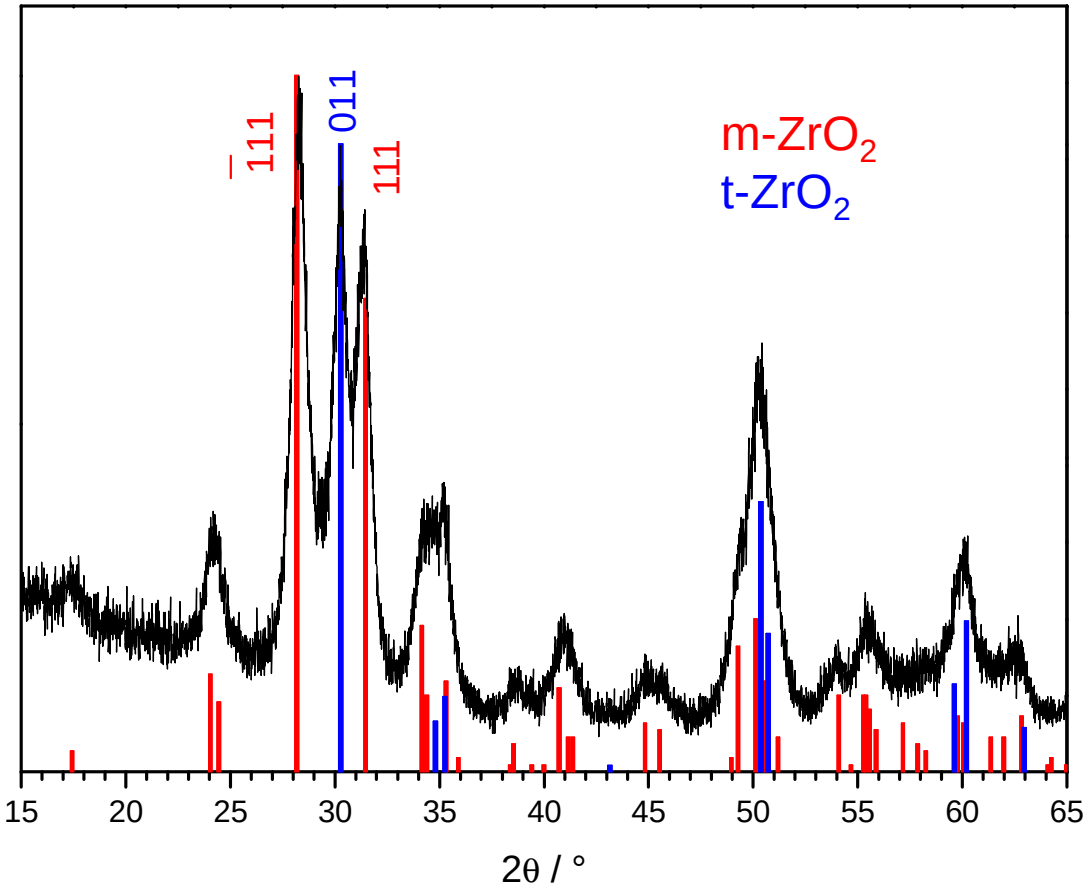

- Pitfalls: Different proportionality factors for scattered intensity

- Two strategies: Pattern fitting or internal standards

- I/I_{cor}: Ratio of the strongest peak of a phase to the strongest peak of corundum in a 1:1 (w/w) mixture

Deviations from the PDF file: Preferred orientation

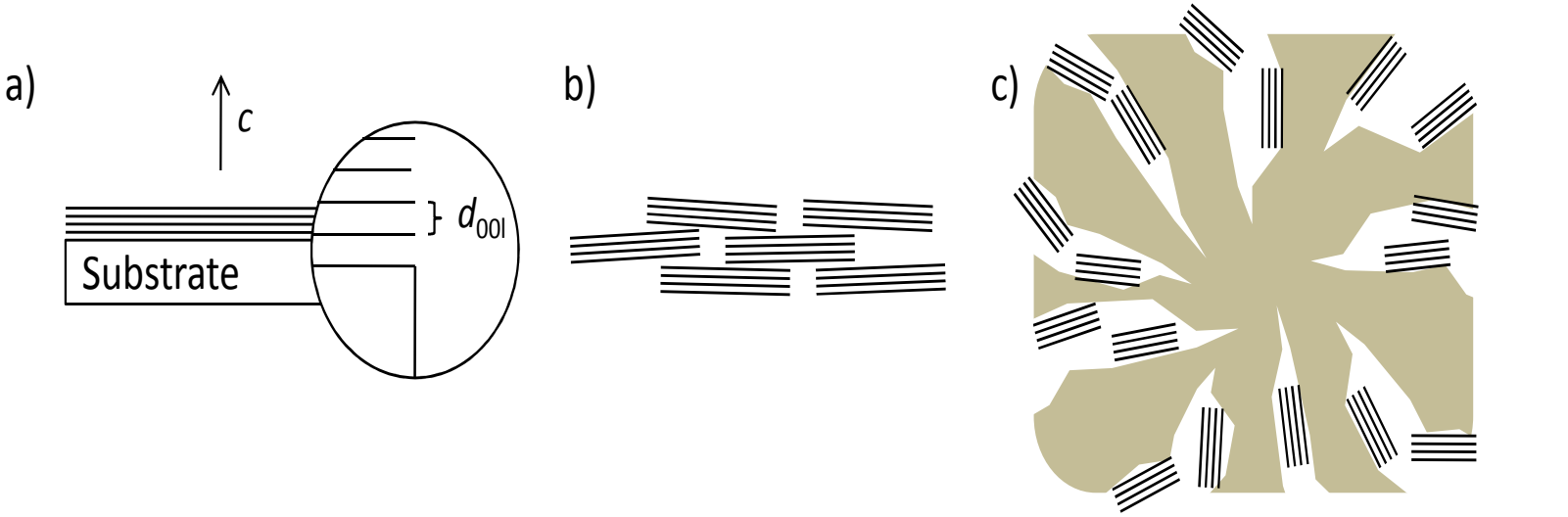

Oriented thin film:
All reflection except
(*00l*) absent

Powder of platelets:
All reflection except
(*00l*) weakened

Supported nano-sized platelets:
No effect of preferred orientation,
but anistropic size effects

Deviations from the PDF file: Chemical variation

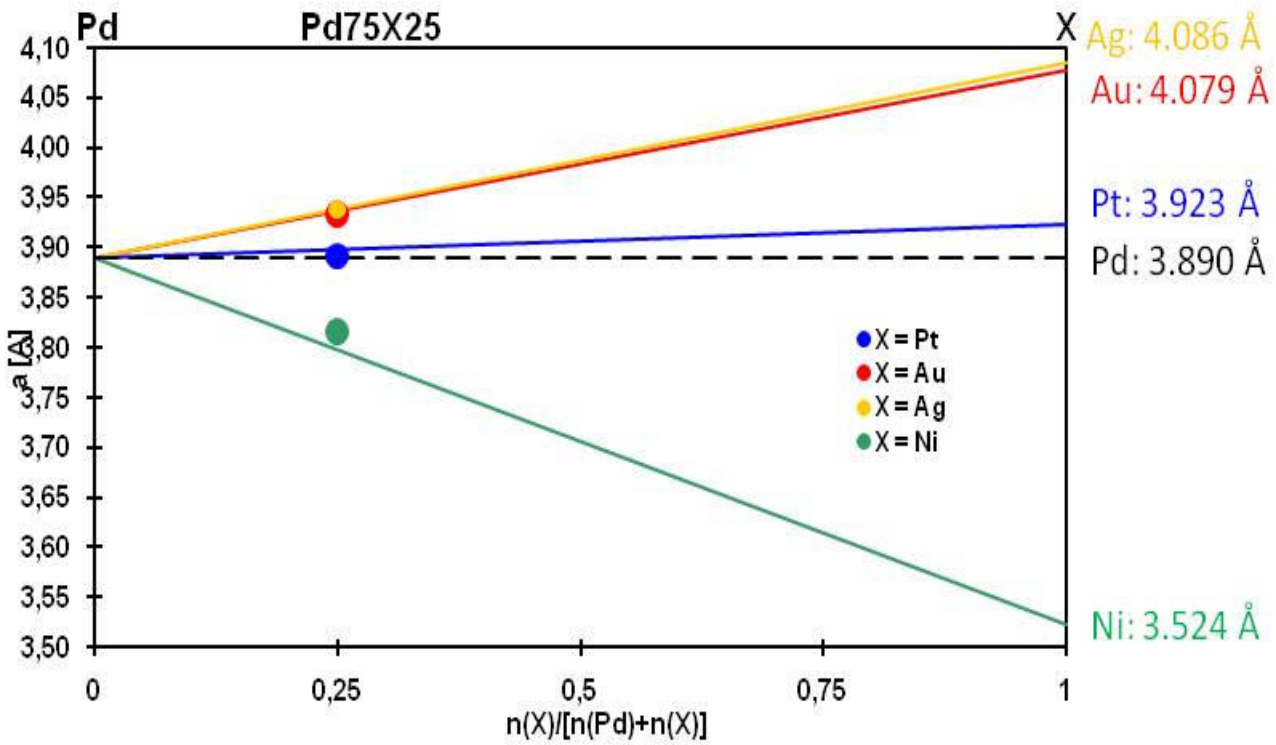

Vegard‘s rule

The Rietveld method

- Whole-pattern-fitting-structure refinement
- Least-squares refinement until the best fit is obtained of the entire powder pattern taken as the whole and the entire calculated pattern
- Simultaneously refined models of crystal structure(s), diffraction optics effects, instrumental factors and other specimen characteristics
- Feedback criteria during refinement
- Pattern decomposition and structure refinement are not separated steps

Procedures in Rietveld refinement

- Experimental data: numerical intensities y_i for each increment i in 2θ
- Simultaneous least-squares fit to all (thousands) of y_i
  - minimize $S_y=\Sigma_i\, y_i^{-1}\,(y_i-y_{ci})^2$
- Expression for y_{ci}

$$y_{ci} = s\,\Sigma_{hkl}\,L_{hkl}\,|F_{hkl}|^2\,\Phi(2\theta_i-2\theta_{hkl})\,P_{hkl}\,A + y_{bi}$$

  - s: scale factor, L_{hkl} contains Lorentz polarization and multiplicity factors, Φ: profile function, P_{hkl} preferred orientation function, A: absorption factor, F_{hkl}: structure factor, y_{bi}: background intensity
- As in all non-linear least-squares refinements, false (local) minima may occur
- Good (near the global minimum) starting models are required

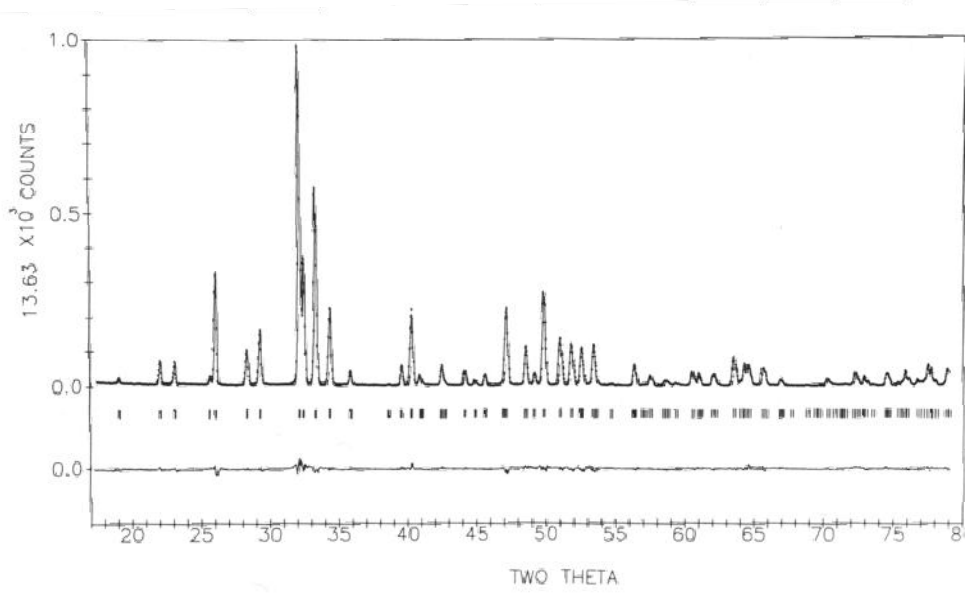

Fig. 1.1 Example of a Rietveld refinement plot. The specimen was fluorapatite. The observed intensity data, y_i, are plotted in the upper field as points with vertical error bars representing the counting statistical e.s.d.'s in them. The calculated pattern is shown in the same field as a solid-line curve. The difference, observed minus calculated, is shown in the lower field. The short vertical bars in the middle field indicate the positions of possible Bragg reflections.

Parameters in Rietveld refinement

- For each phase
  - x_j y_j z_j B_j N_j (Position, isotropic thermal parameter and site occupancy of the jth atom in the unit cell
  - Scale factor
  - Profile breadth parameters (2θ dependence of FWHM, typically Cagliotti function $FWHM^2 = U \tan^2\theta + V \tan\theta + W$)
  - Lattice parameters
  - Overall temperature factor
  - individual anisotropic temperature factors
  - Preferred orientation
  - Extinction
- Global parameters
  - 2θ-Zero
  - Instrumental profile (+ asymmetry)
  - Background (several parameters in analytical function)
  - Wavelength
  - Specimen displacement, transparancy
- Altogether some 10-100 parameters: Keep an eye on the refined parameters-to-reflections (independent observations) ratio to avoid over-fitting

Criteria of fit

- R-Bragg

$$R_B = \frac{\Sigma \left| I_K("obs") - I_K(calc) \right|}{\Sigma I_K("obs")}$$

  - insensitive to misfits not involving the Bragg intensities of the phase(s) being modelled

- R weighted pattern

$$R_{wp} = \left(\frac{\Sigma w_i (y_i(obs) - y_i(calc))^2}{\Sigma w_i (y_i(obs))^2} \right)^{1/2}$$

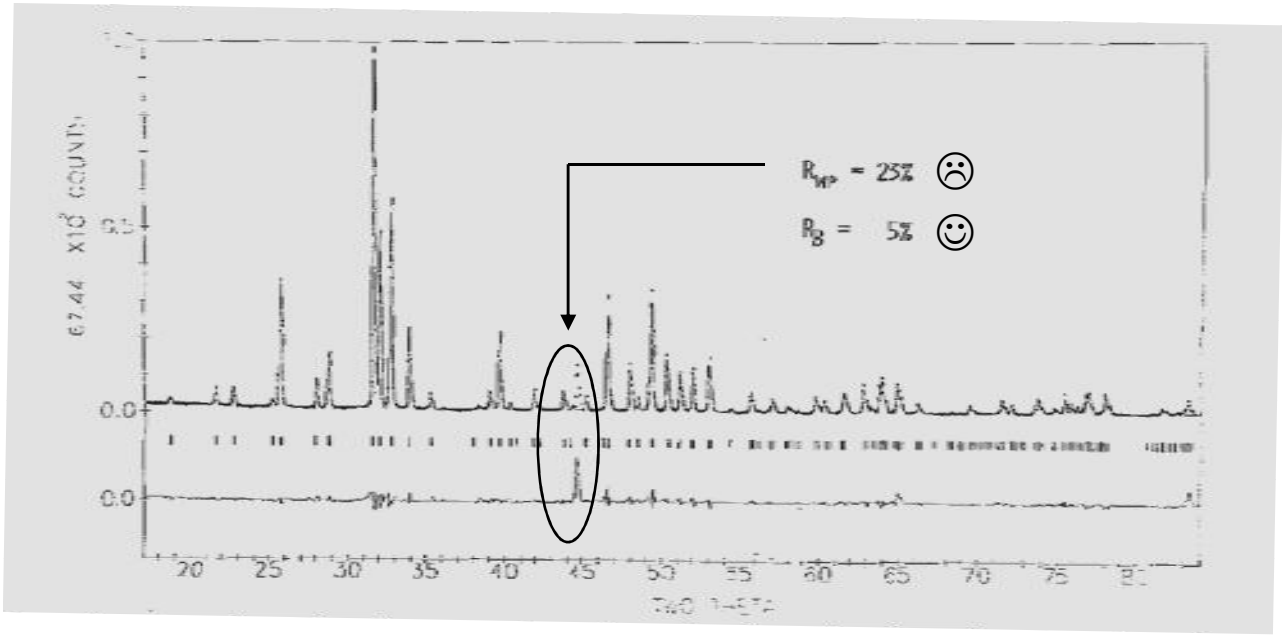

Example: M1 oxidation catalyst

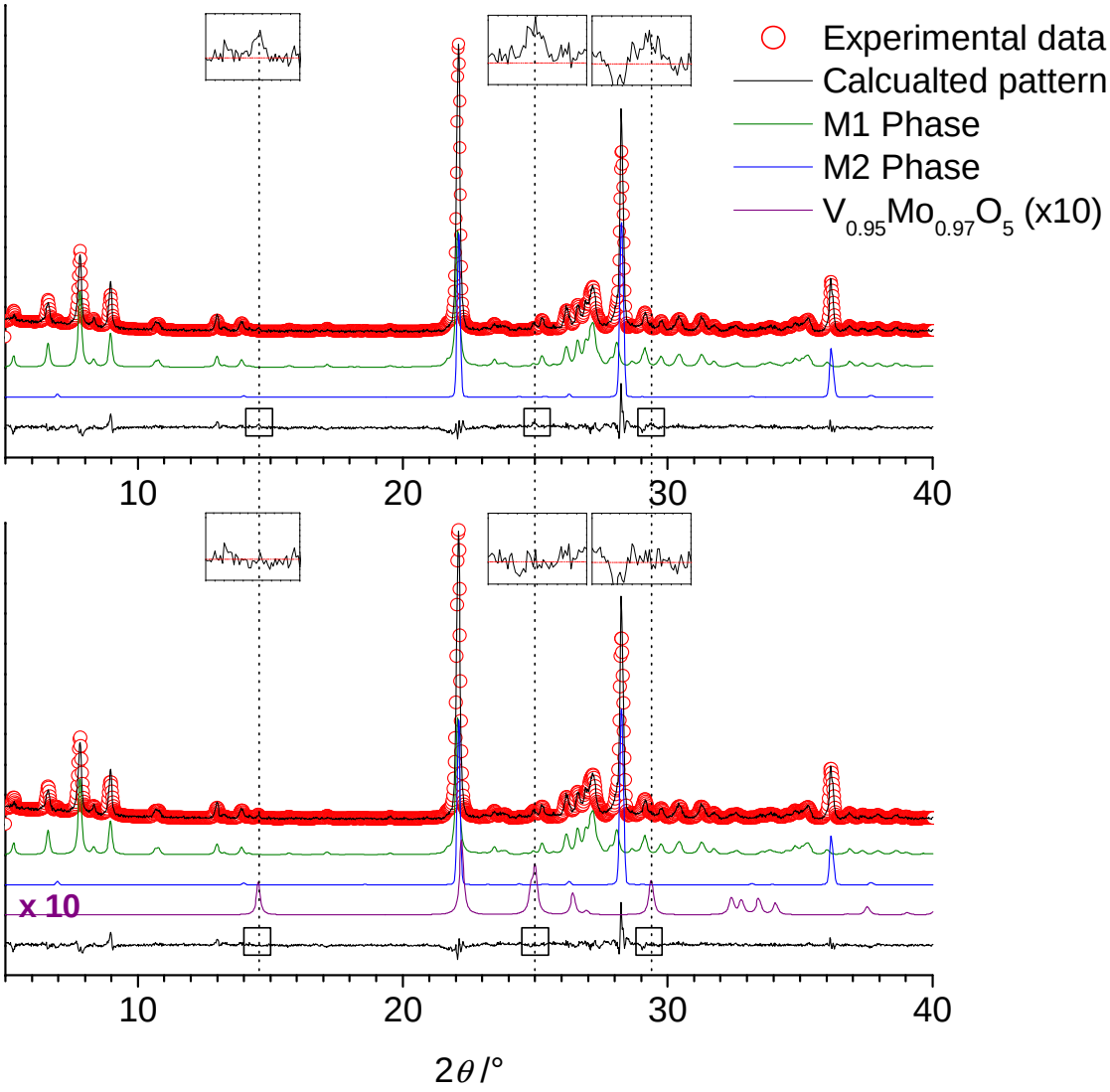

$MoVTeNbO_x$

Example: Cu/ZnO catalyst precursors

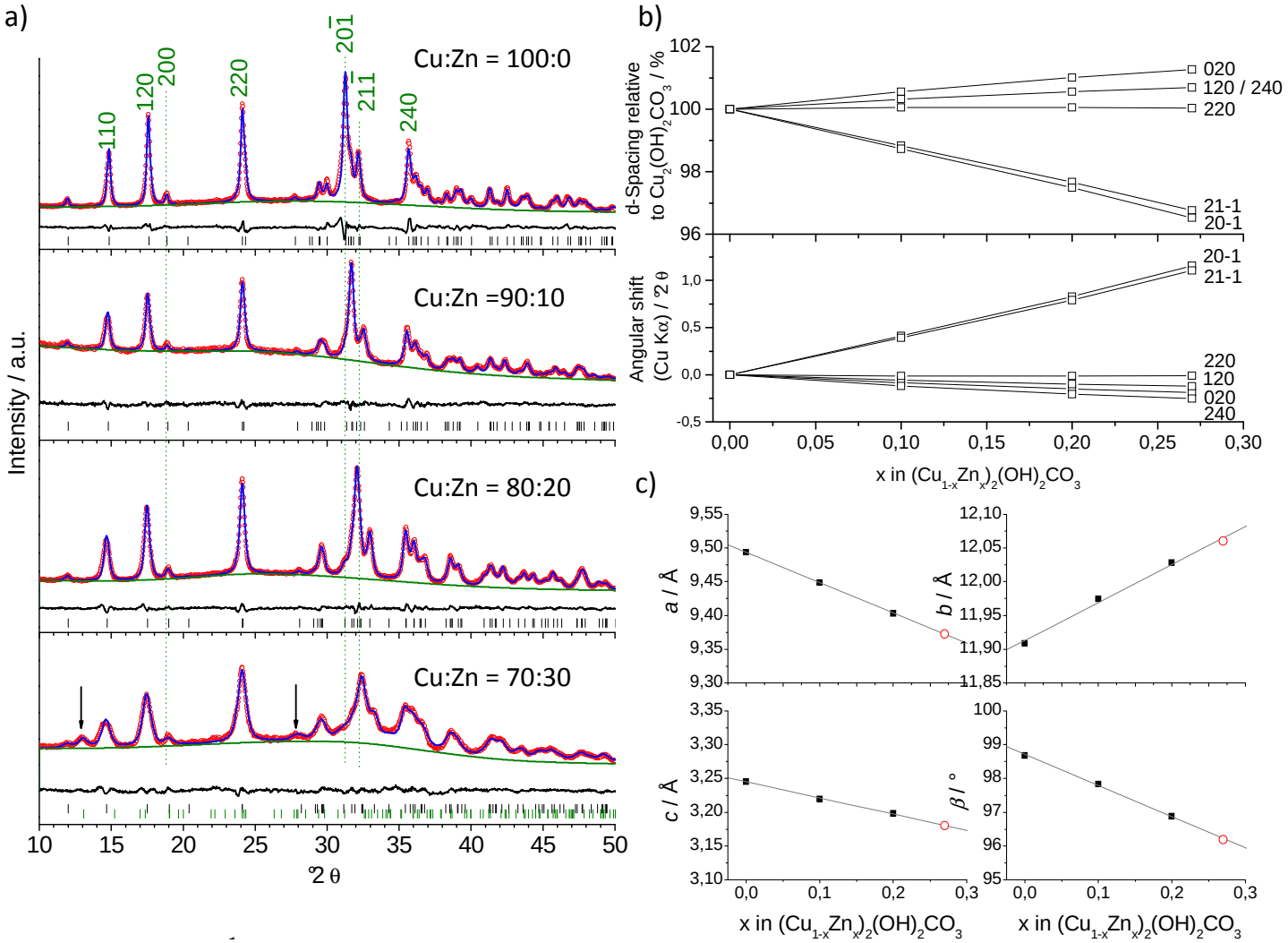

Real structure: Line profile analysis

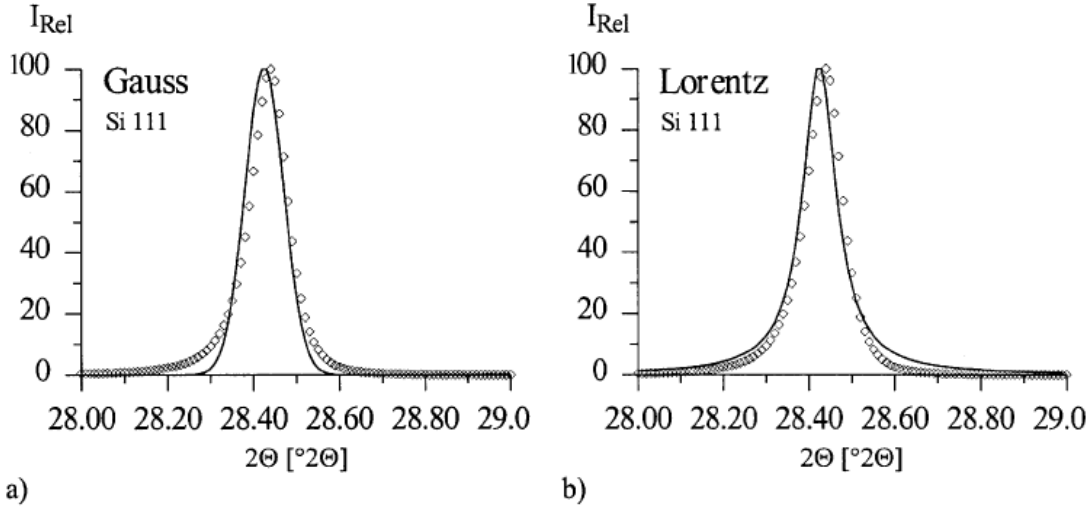

- Fitting of a suitable profile function to the experimental data
  - Gauss, Lorentz, Pseudo-Voigt, Pearson-VII
- No structural model
- Parameters for each reflection:
  - angular position (2θ)
  - maximal intensity I_{max}
  - integral intensity A
  - FWHM or integral breadth $\beta = A / I_{max}$
  - profile paramter (P7: m, pV: η)
- Patterns of high quality and with low overlap of peaks are required

Instrumental contribution

- Line width dominated by beam divergence and flat-sample-error (low 2θ), slits (medium 2θ) and wavelength distribution in spectrum of XRD tube (high 2θ)
- Peaks of standard sample (large crystals, no strain, similar to sample, same measurement conditions) can be extrapolated by fitting a Cagliotti function

$$FWHM^2 = U \tan^2\theta + V \tan\theta + W$$

Instrumental resolution function

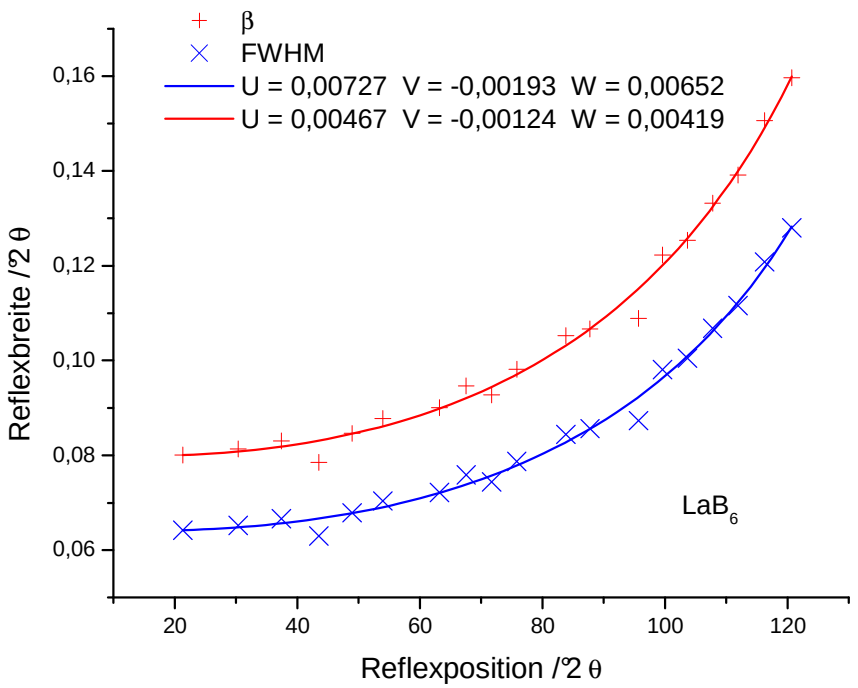

Sample line broadening

- Size effect
  - incomplete destructive interference at $\theta_{Bragg} \pm \Delta\theta$ for a limited number of lattice planes
  - detectable for crystallites roughly < 100 nm
  - no 2θ dependence

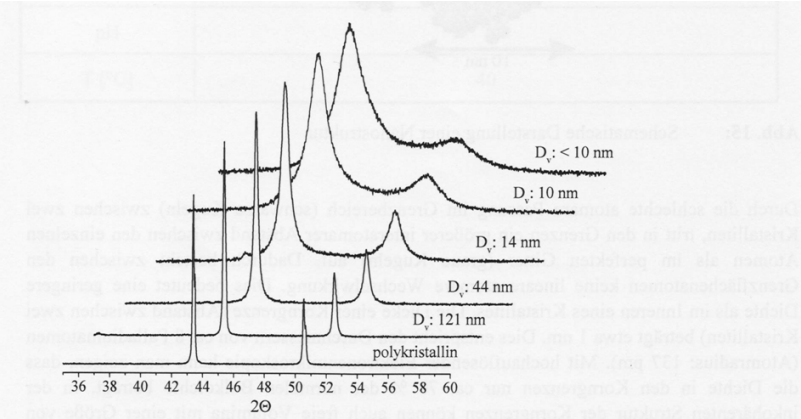

Abb. 16: 111- und 200-Reflex von Kupferproben mit unterschiedlicher Teilchengröße

- Strain effect
  - variation in d
  - introduced by defects, stacking fault, mistakes
  - depends on 2θ

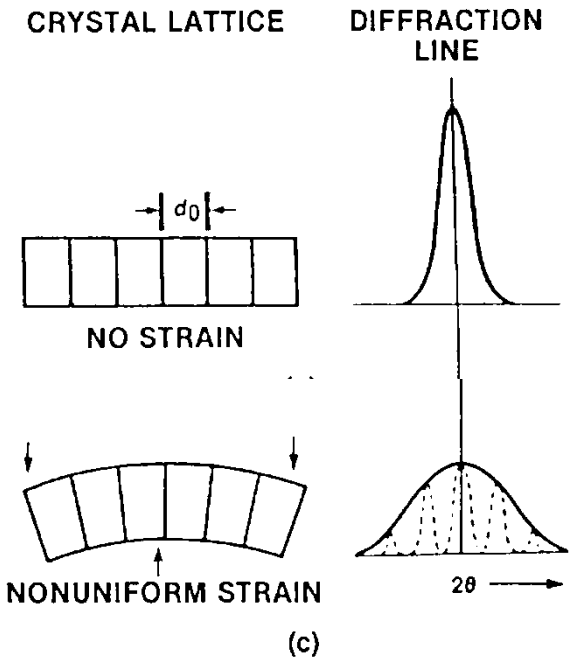

The term strain

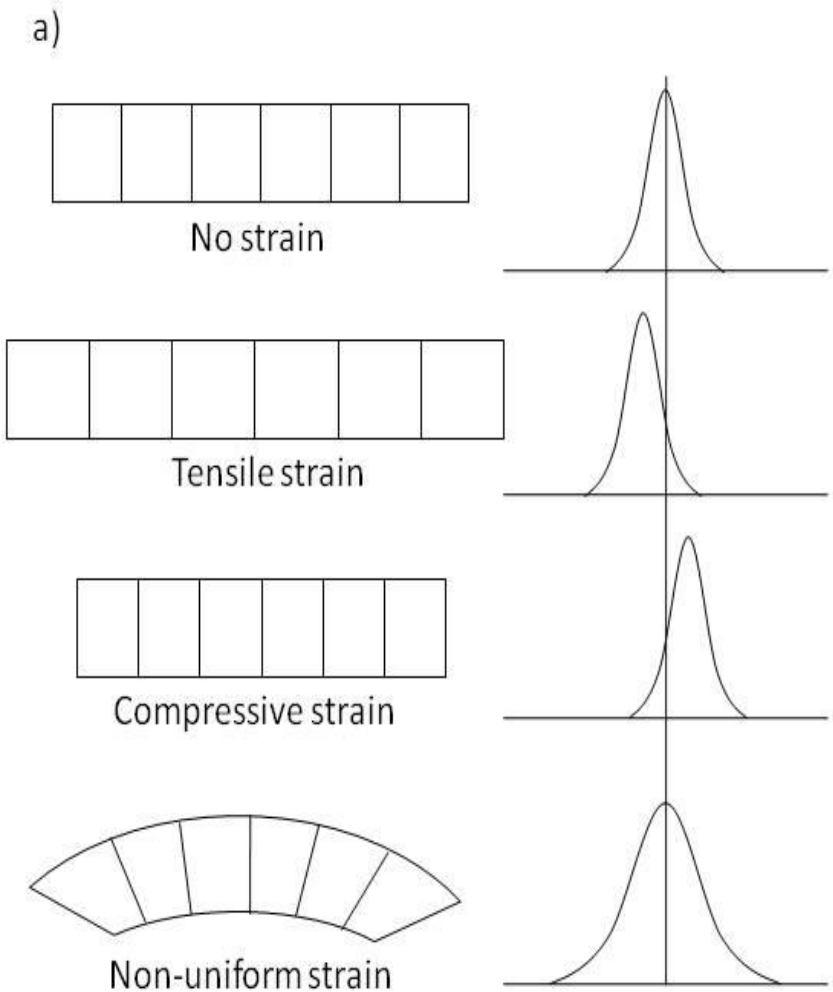

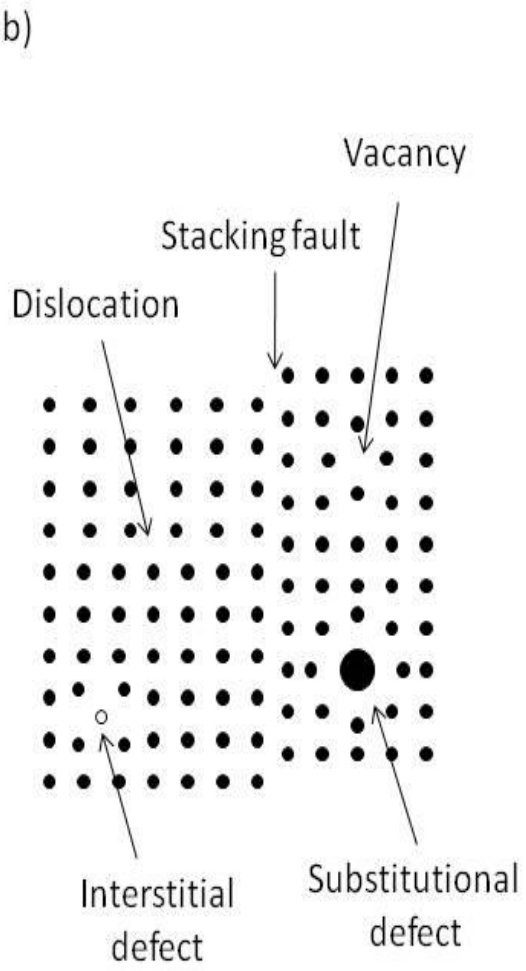

Micro- or lattice strain:

$\Delta d / d$

The term size

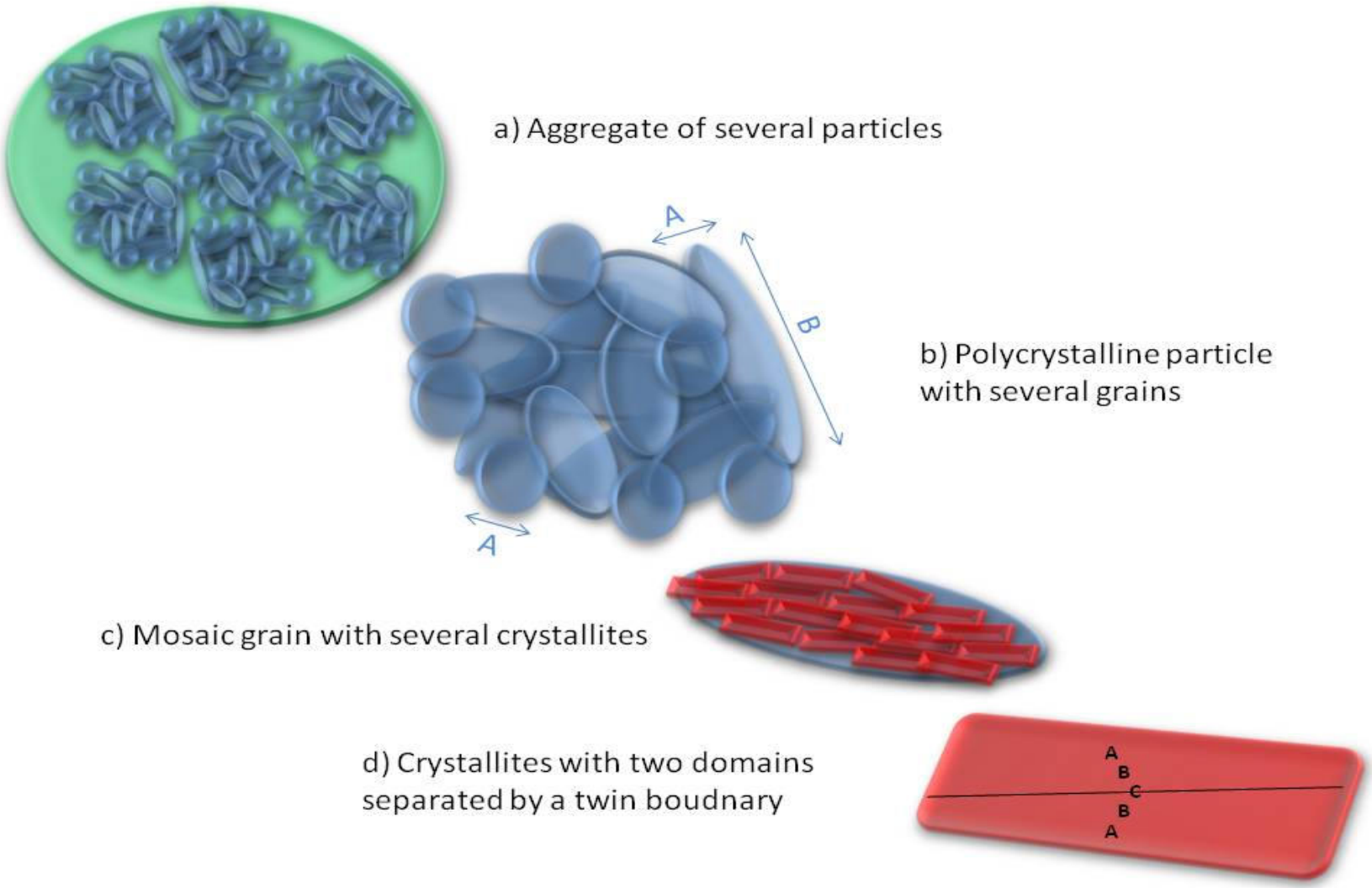

Scherrer equation

- Determination of size effect, neglecting strain (Scherrer, 1918)
- Thickness of a crystallite $L = N\, d_{hkl}$

  $L_{hkl} = k\,\lambda / (\beta \cos\theta)$,

  β has to be corrected for instrumental contribution:

  $\beta^2 = \beta^2_{obs} - \beta^2_{standard}$

  (for Gaussian profiles)

  – k: shape factor, typically taken as unity for β and 0.9 for FWHM
- Drawbacks: strain not considered, physical interpretation of L, no information on size distribution, works best for L < 5 nm (not for L > 100 nm)

Wilson equation

- Determination of strain, neglecting size effects (Stokes & Wilson, 1944)
- $\beta = 4\varepsilon \tan\theta$

  β has to be corrected for instrumental contribution:

  $\beta^2 = \beta^2_{obs} - \beta^2_{standard}$

  (for Gaussian profiles)
- Drawbacks: size not considered

- In reality often:

  $\beta_{obs} = \beta_{instr} + \beta_{sample} = \beta_{instr} + \beta_{size} + \beta_{strain}$

Pattern decomposition

- β_{size}, β_{strain} and β_{instr} contribute to β_{obs}
- Correction for β_{instr} from IRF
- Reciprocal quantities for each reflection

  - $\beta^* = \beta \cos \theta / \lambda$
  - $|d^*| = 1 / d = 2 \sin \theta / \lambda$

Wiliamson-Hall analysis

- Indexed plot of β* vs d*
  - Horizontal line: no strain, isotropic size effect
  - Horizontal lines for higher order reflections: no strain, anisotropic size effect
  - Straight line through the origin: isotropic strain
  - Straight line for higher order reflections but different slopes: anisotropic strain

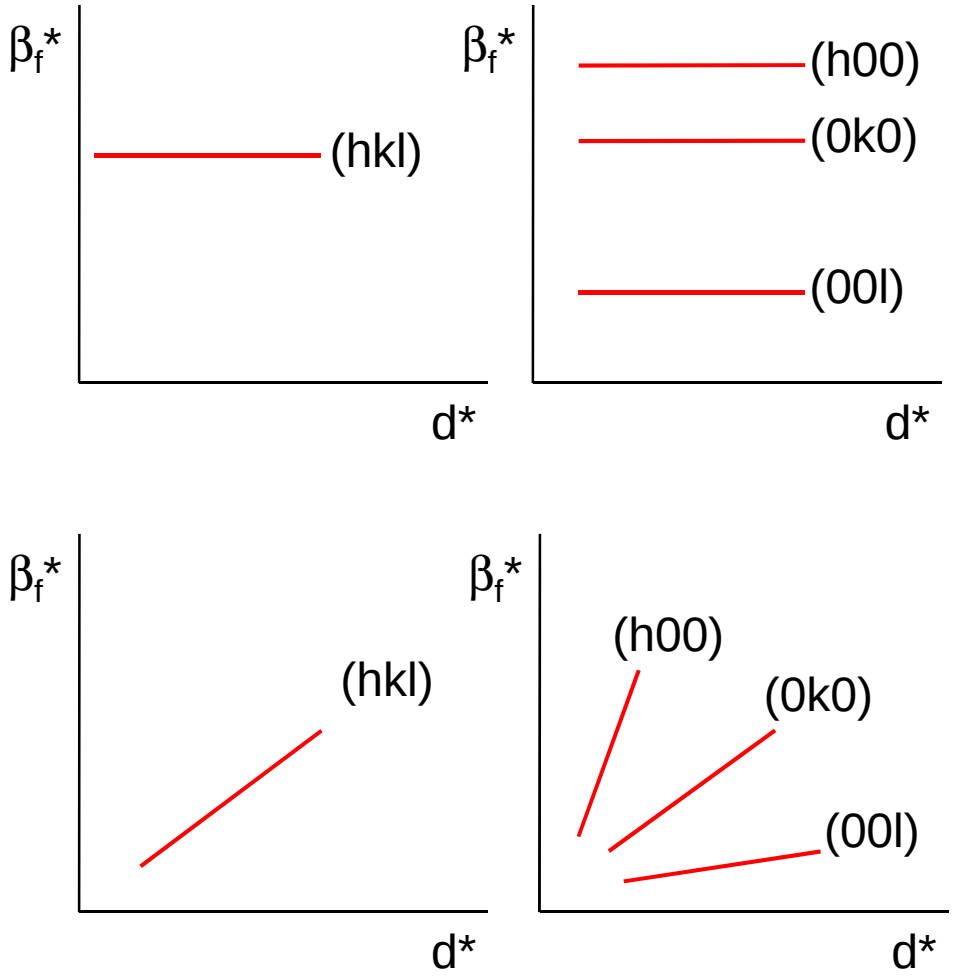

Example WH-analysis: ZnO

- ZnO obtained by thermal decomposition of $Zn_3(OH)_4(NO_3)_2$

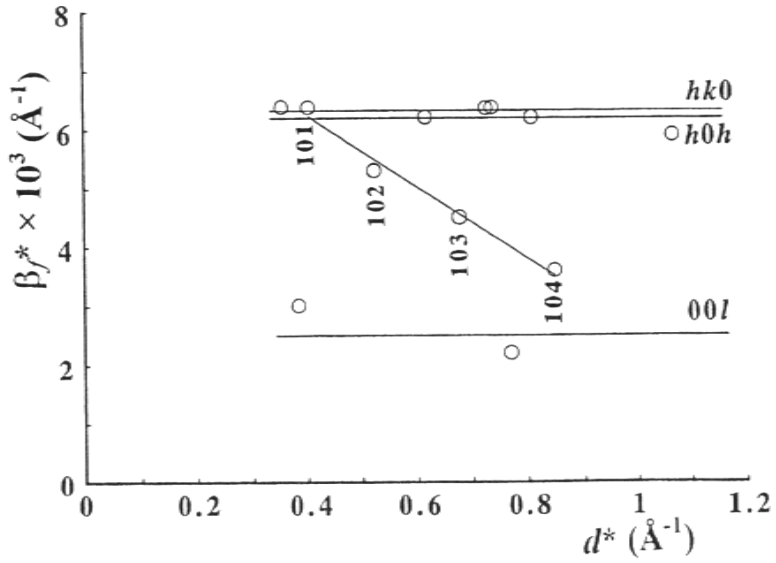

Fig. 28.7. Williamson–Hall plot for strain-free ex-hydroxide-nitrate ZnO.

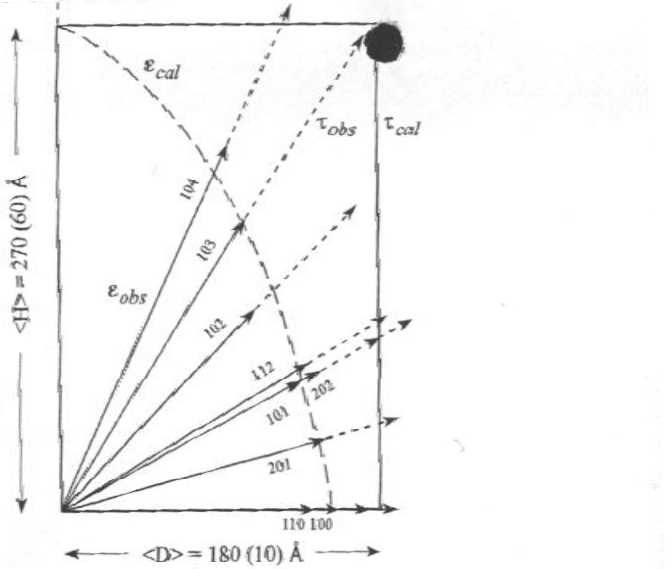

Fig. 28.8. Section through the 'average' cylinder (τ_{cal}) used to model the form of the crystallites of the ex-hydroxide-nitrate ZnO sample. —→: observed apparent size ε_{obs}, – – – →: actual observed size τ_{obs} in the direction *hkl*, the dotted curve is the loci of the calculated apparent sizes (from Langford *et al.*, 1993).

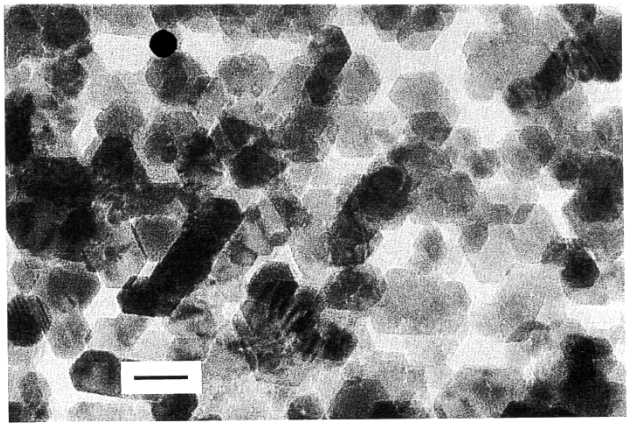

Fig. 28.9. TEM micrograph of ex-hydroxide-nitrate ZnO showing hexagonal crystallites (bar = 200 Å).

J. I. Langford, A. Boultif, J. P. Auffrédic, D. Louër, *J. Appl. Crystallogr.* 1993, 26, 22.

Example: Peak sharpening of a PdGa hydrogenation catalyst

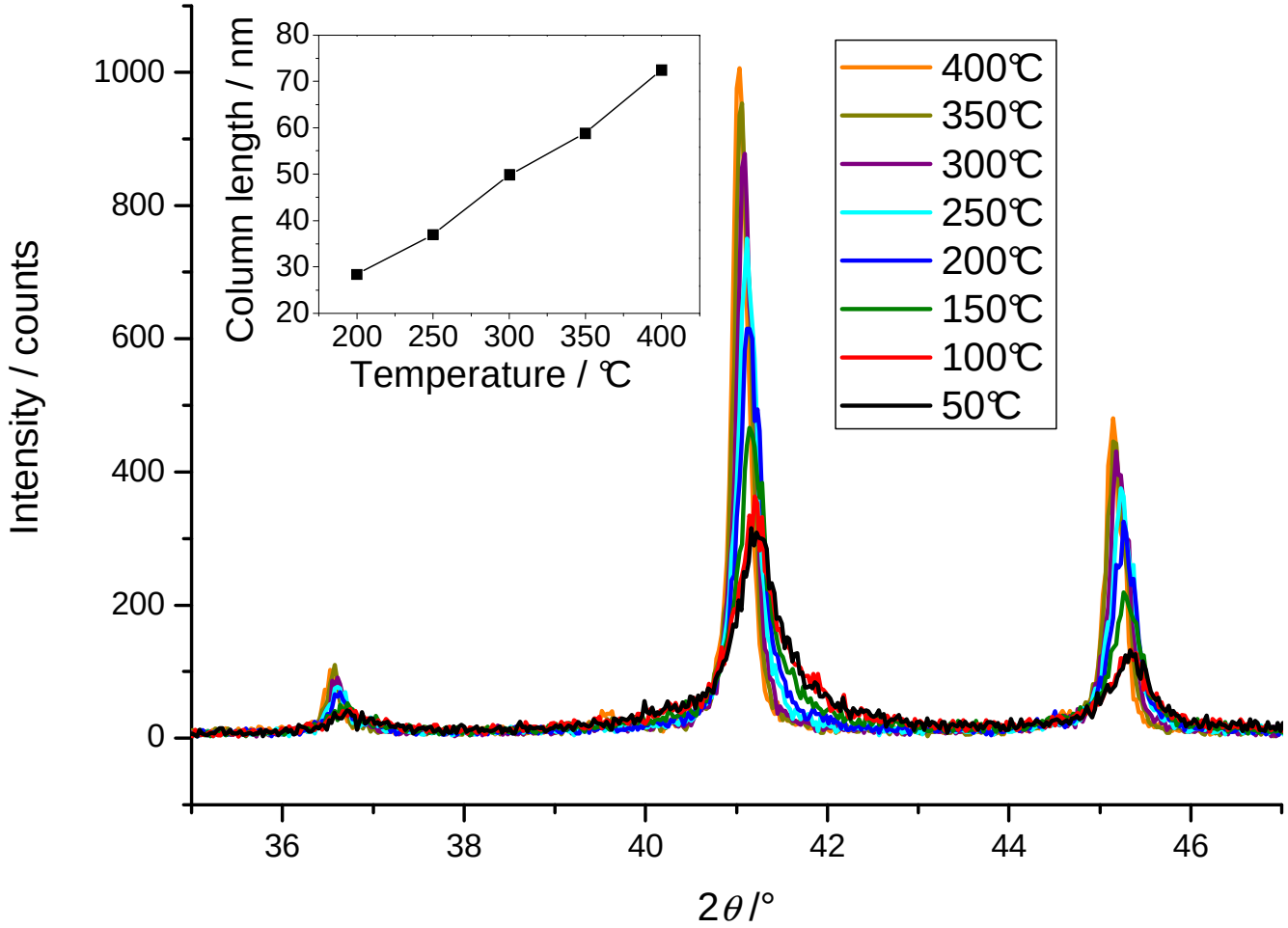

Example: Microstructure of catalysts

TEM-size:
4-6 nm

XRD-size:
1-2 nm

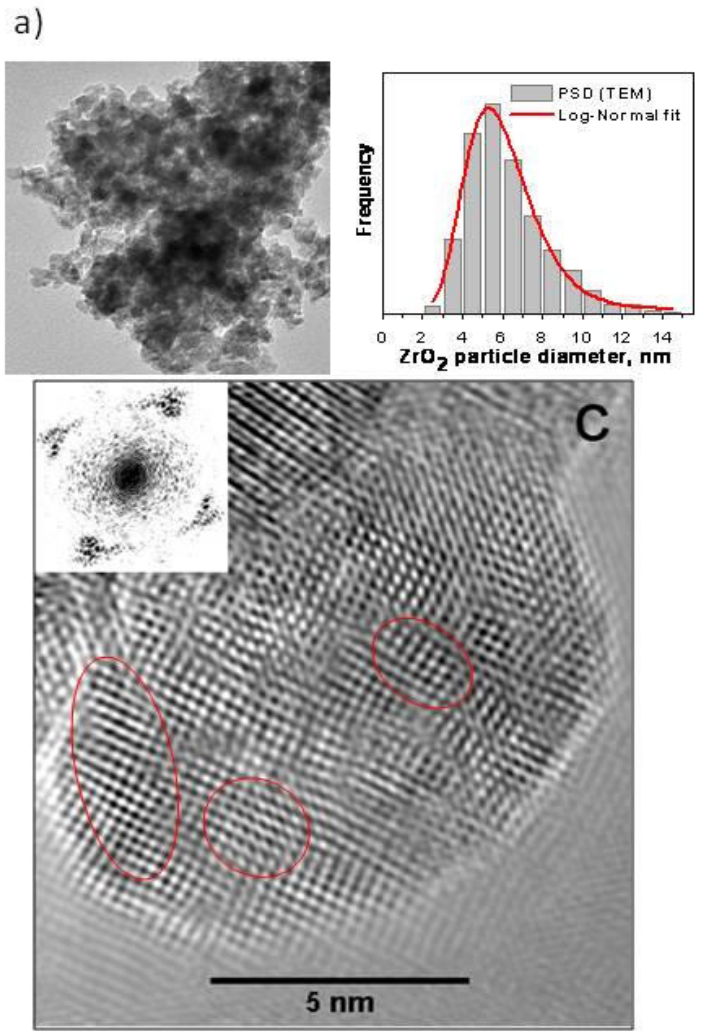

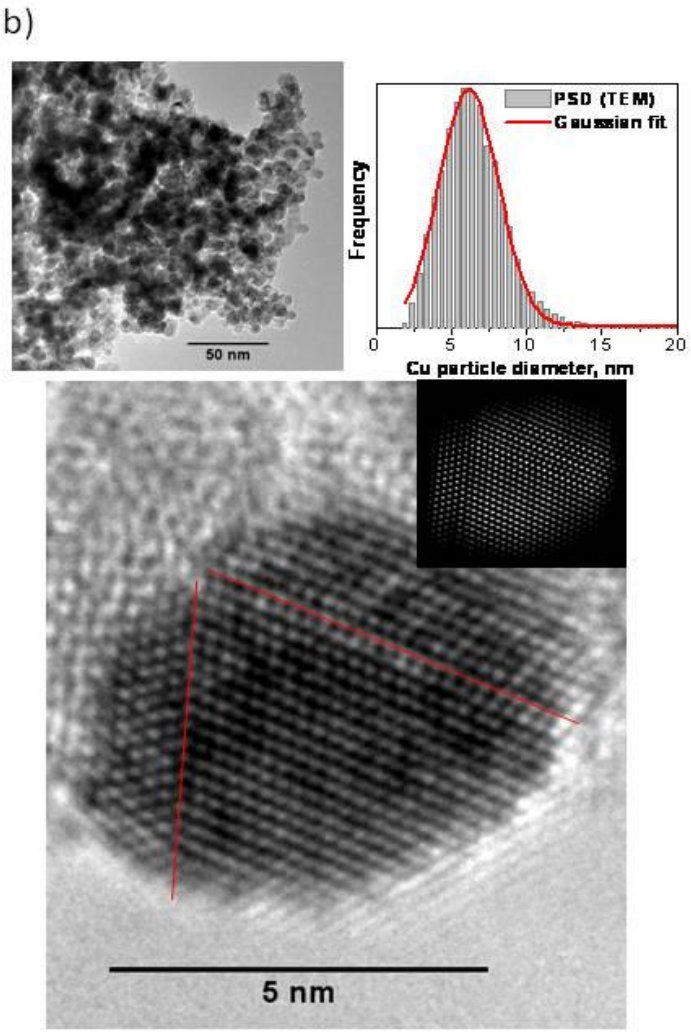

TEM-size:
7-8 nm

XRD-size:
3-4 nm

Neutrons

- According to the wave-particle dualism (λ = h/mv, de Broglie) neutrons have wave properties
- As X-rays neutrons may have a wavelength on the order of the atomic scale (Å) and a similar interaction strength with matter (penetration depth from µm to many cm)
- Neutrons generate interference patterns and can be used for Bragg diffraction experiments
- Same scattering theory for neutrons and X-rays

Generation of neutrons

- Neutron must be released from the atomic nuclei, two possibilities:
  - Fission reactor
    - ^{235}U nuclei break into lighter elements and liberate 2 to 3 neutrons for every fissioned element

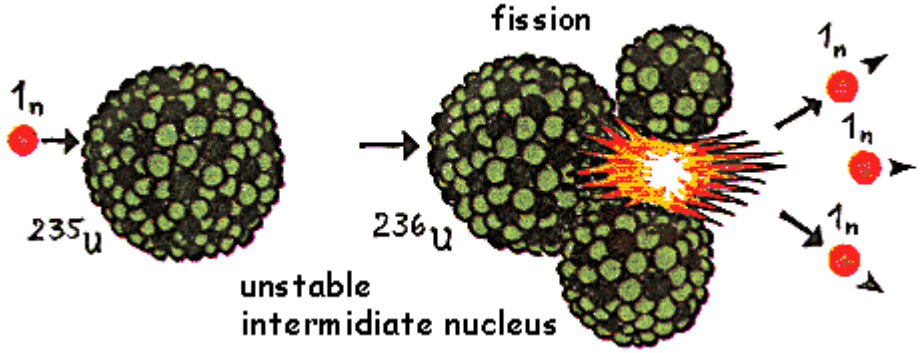

www.hmi.de

  - Spallation source
    - proton bombardment of lead nuclei, releasing spallation neutrons

Research reactor at Helmholtz Zentrum Berlin

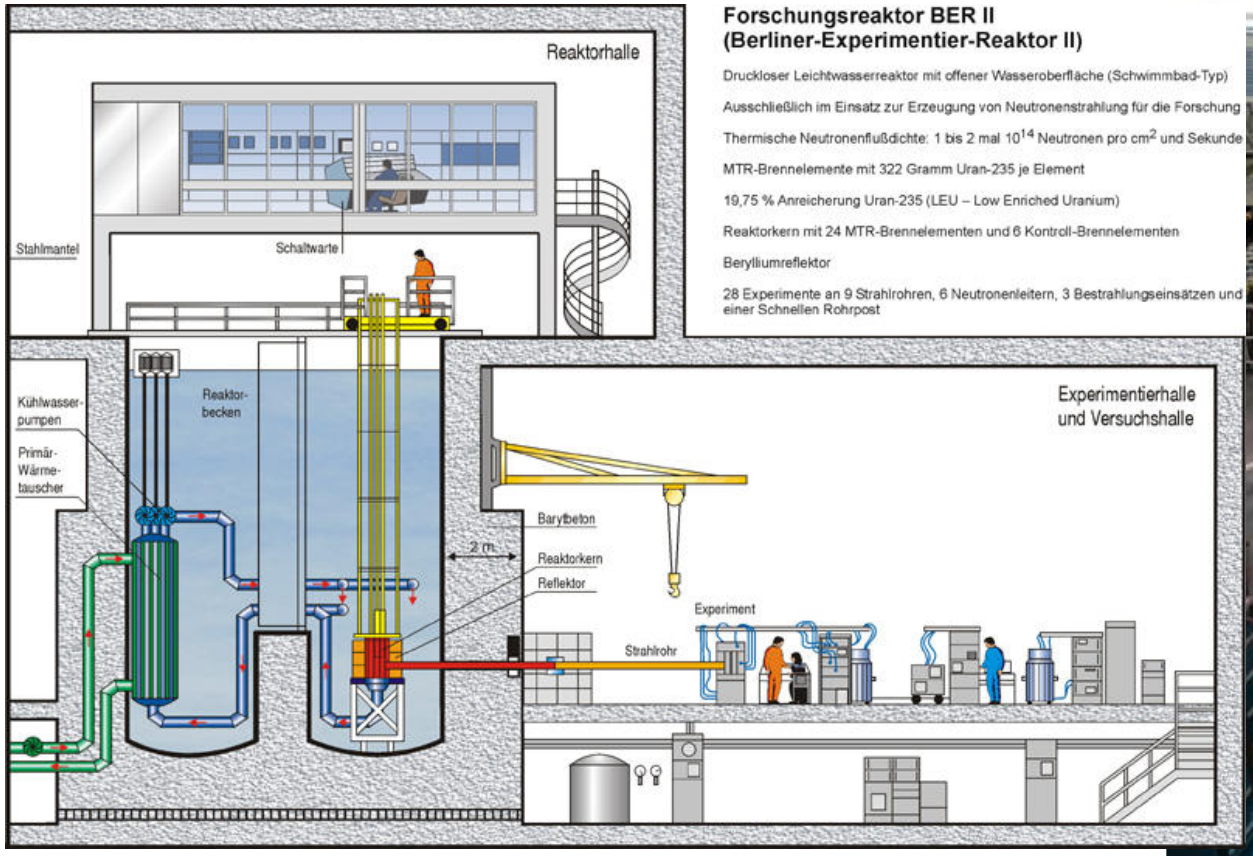

Forschungsreaktor BER II (Berliner-Experimentier-Reaktor II)

Druckloser Leichtwasserreaktor mit offener Wasseroberfläche (Schwimmbad-Typ)

Ausschließlich im Einsatz zur Erzeugung von Neutronenstrahlung für die Forschung

Thermische Neutronenflußdichte: 1 bis 2 mal 10^{14} Neutronen pro cm^2 und Sekunde

MTR-Brennelemente mit 322 Gramm Uran-235 je Element

19,75 % Anreicherung Uran-235 (LEU – Low Enriched Uranium)

Reaktorkern mit 24 MTR-Brennelementen und 6 Kontroll-Brennelementen

Beryllumreflektor

28 Experimente an 9 Strahlrohren, 6 Neutronenleitern, 3 Bestrahlungseinsätzen und einer Schnellen Rohrpost

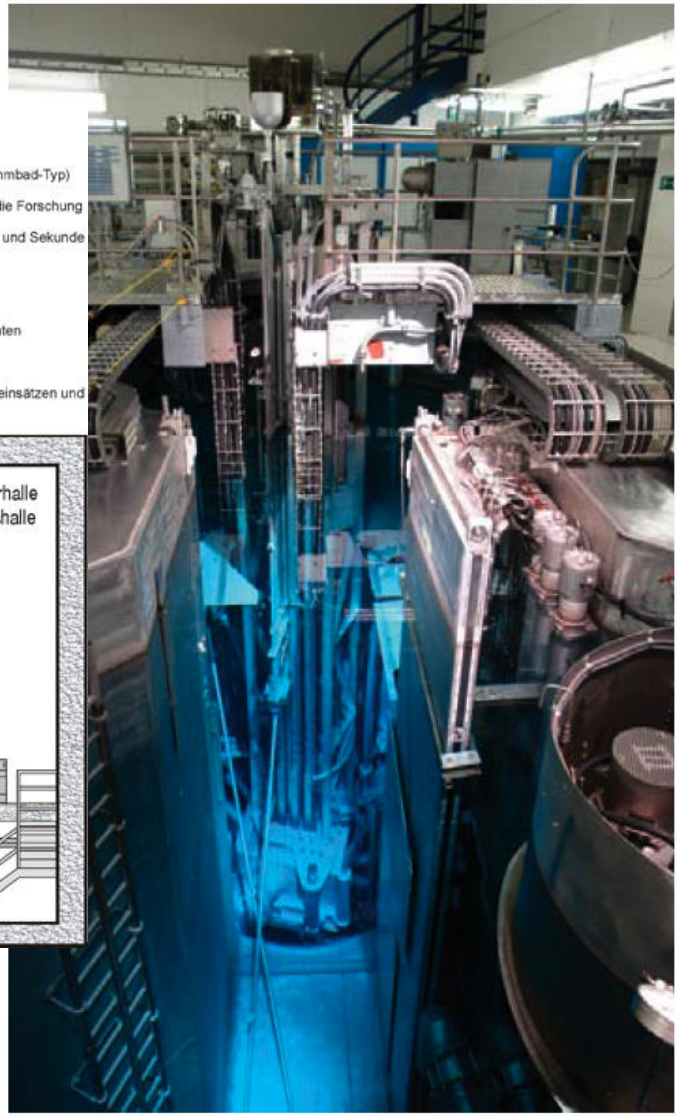

www.hmi.de

Properties of neutrons

- Fission process: 1 MeV – too high for practical use
- Neutrons are slowed down (moderated in water or carbon)
  - hot neutrons:
    - moderated at 2000°C
    - 0.1-0.5 eV, 0.3-1 Å, 10 000 m/s
  - thermal neutrons:
    - moderated at 40℃
    - 0.01-0.1 eV, 1-4 Å, 2000 m/s
  - cold neutrons:
    - moderated at -250°C
    - 0-0.01 eV, 0-30 Å, 200 m/s

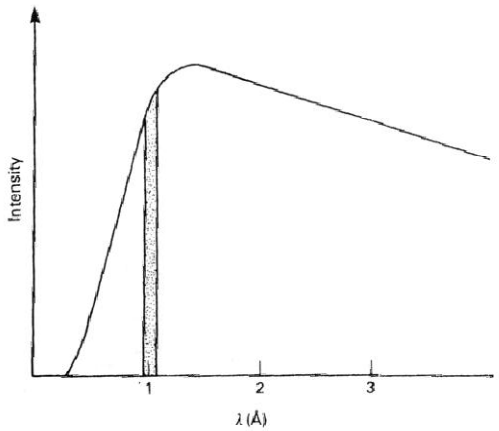

Fig. 2.16. Spectral distribution of moderated neutrons from a nuclear reactor. A narrow band of wavelengths can be selected for diffraction experiments.

Neutrons vs. X-rays

- Particle wave
- Mass, Spin 1/2, Magnetic dipole moment
- Neutrons interact with the nucleus
- Scattering power independent of 2θ

- Electromagnetic wave
- No mass, spin 1, no magnetic dipole moment
- X-ray photons interact with the electrons
- Scattering power falls off with 2θ

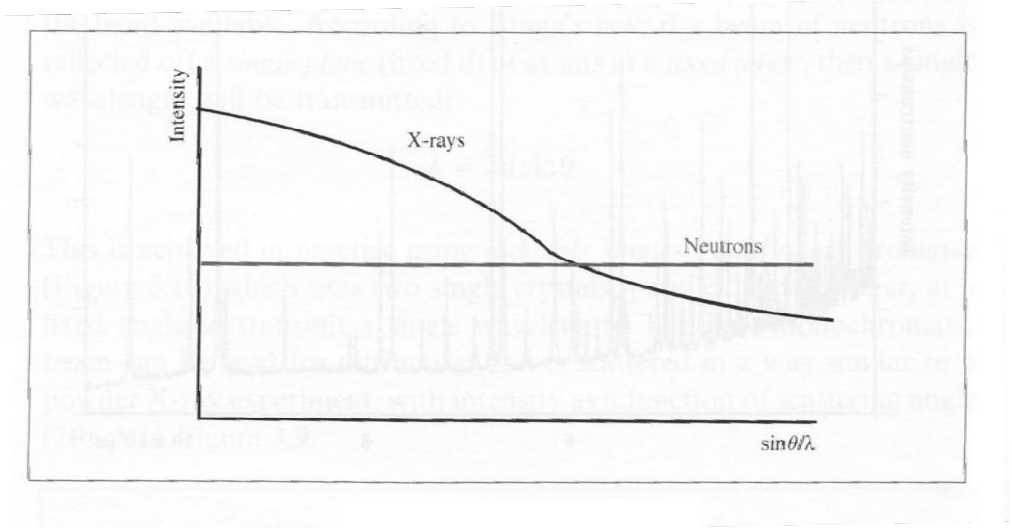

Figure 3.16 Variation of scattering amplitude with angle

Scattering lengths

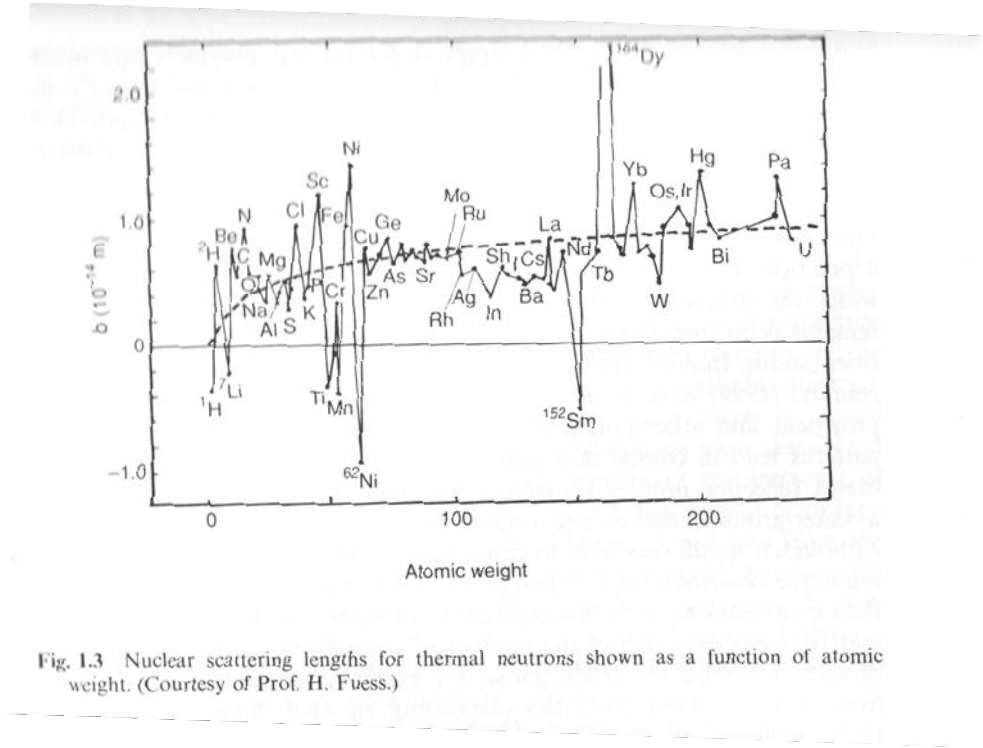

Fig. 1.3 Nuclear scattering lengths for thermal neutrons shown as a function of atomic weight. (Courtesy of Prof. H. Fuess.)

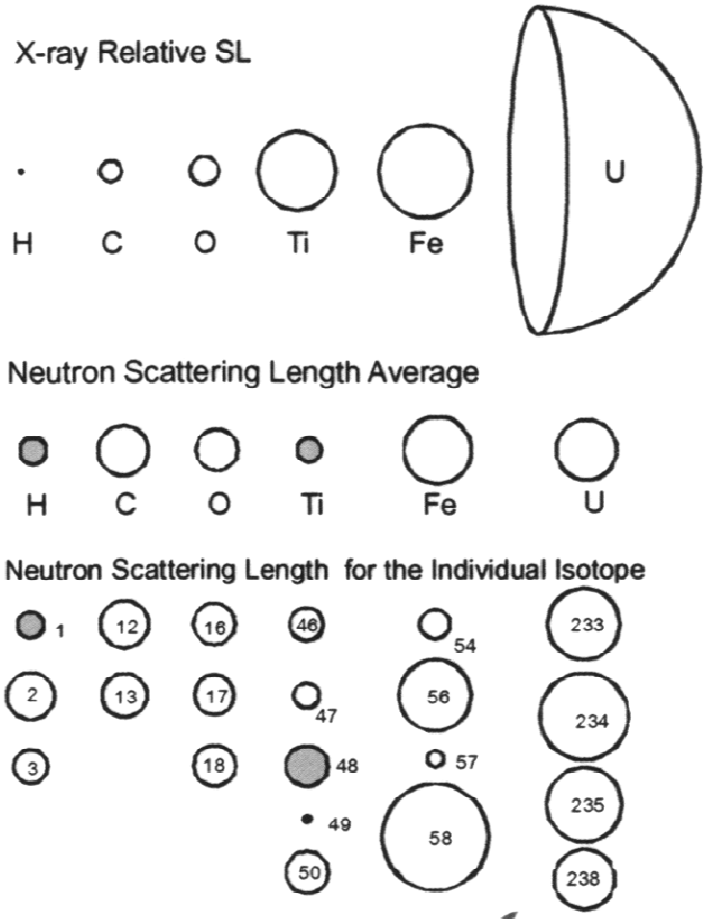

Neutron vs. XRD pattern

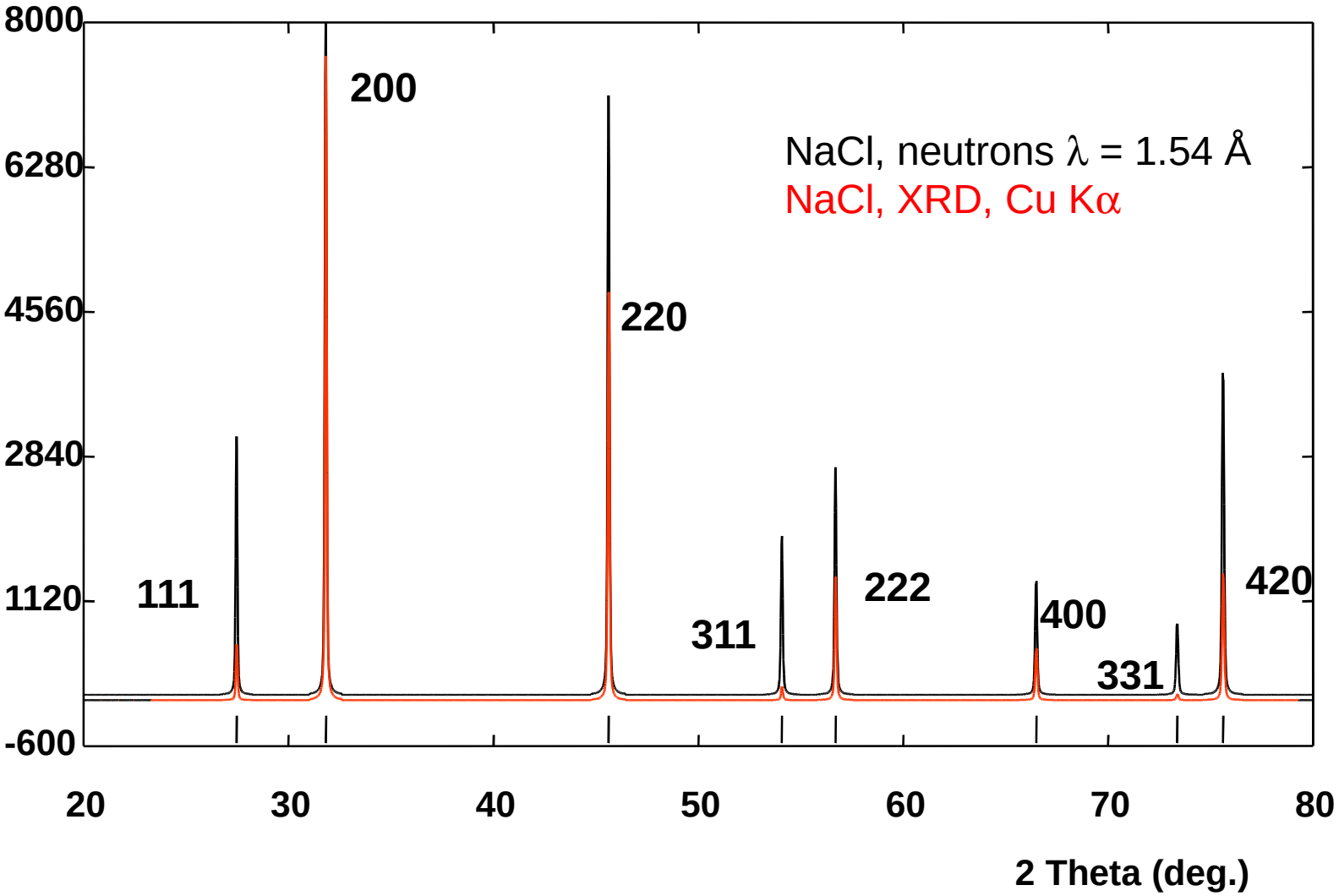

Neutrons vs. X-rays

- Lower absorption
- Large amounts of sample needed
- Neighbors and isotopes can be discriminated
- Light elements can be seen
- Low availability (nuclear reactor)
- Magnetic structures can be investigated
- Incoherent scatterers (eg. H) have to be avoided

- Stronger absorption
- Lower amounts of sample needed
- Neighbors and isotopes cannot be discriminated
- Light elements hard to detect
- High availability (lab instrument)

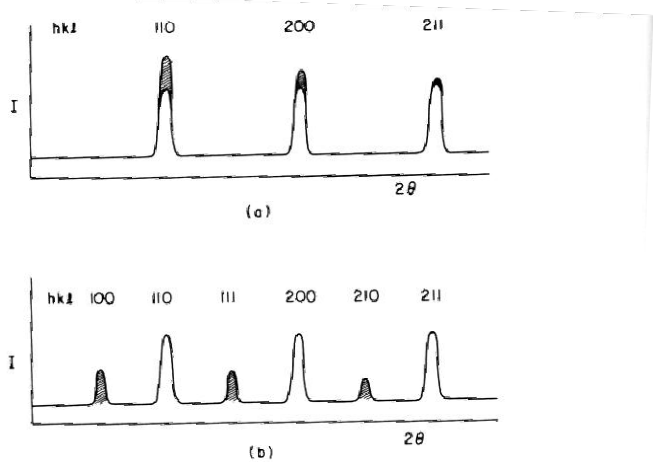

FIG. 4-27. Schematic neutron diffraction patterns from polycrystalline (a) bcc ferromagnet and (b) bcc antiferromagnet. The shaded area represents the contribution of the magnetic scattering which decreases with θ due to the decrease in magnetic scattering factor f_{mag}.

Defect analysis of fcc Cu catalysts

M.S. Paterson, J. Appl. Phys. 23, 1952, 805: (h+k+l = 3N±1) broadened and shifted; (h+k+l = 3N) not affected

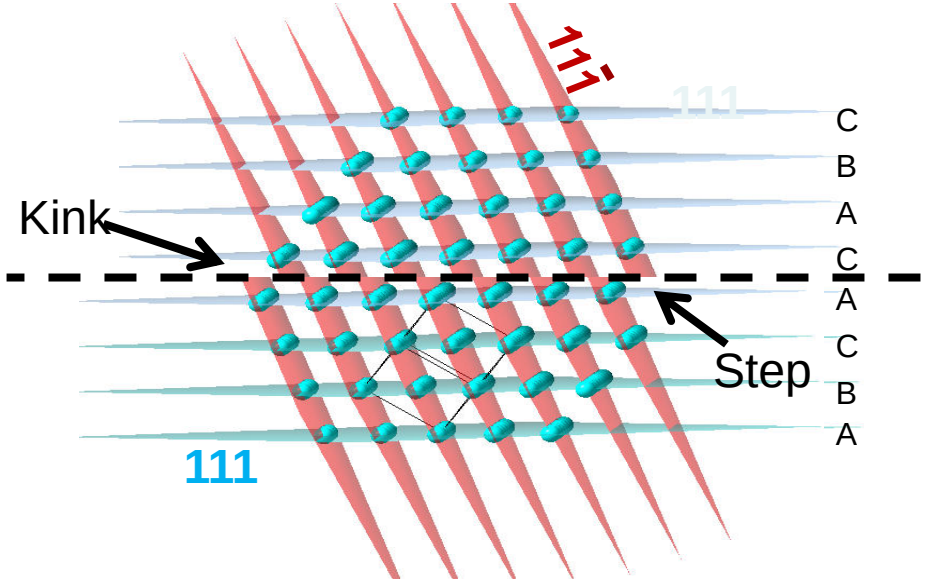

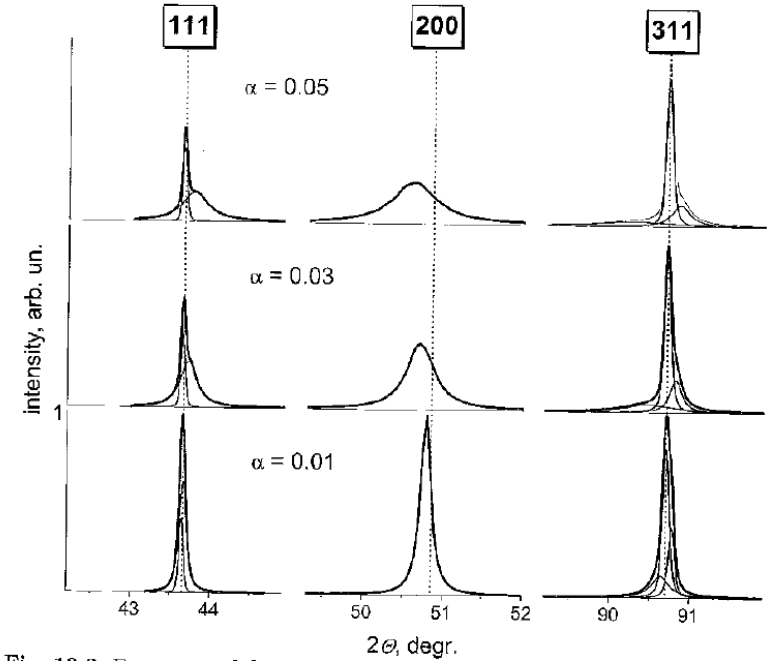

Example: Stacking faults in Cu catalysts

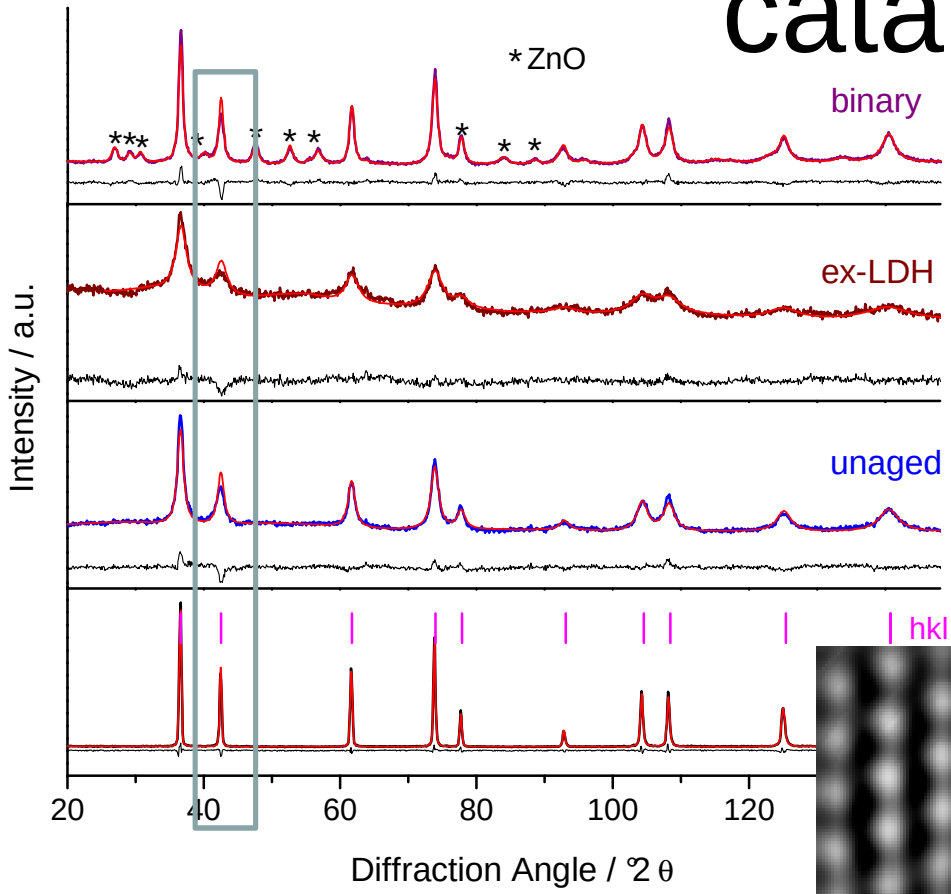

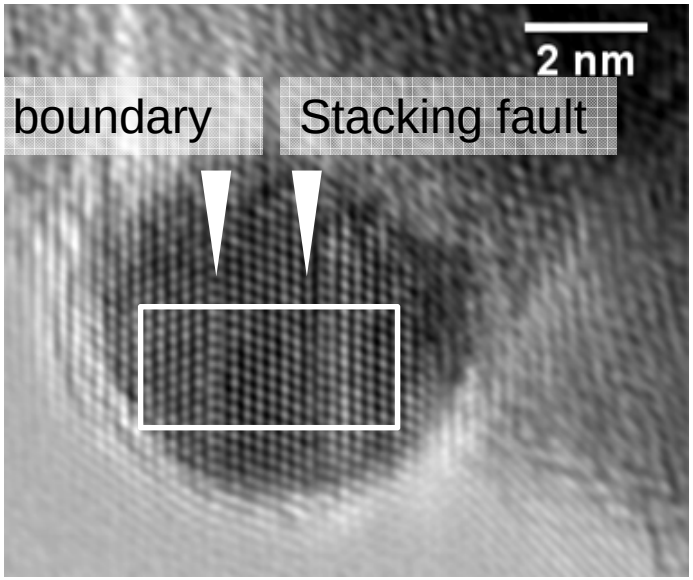

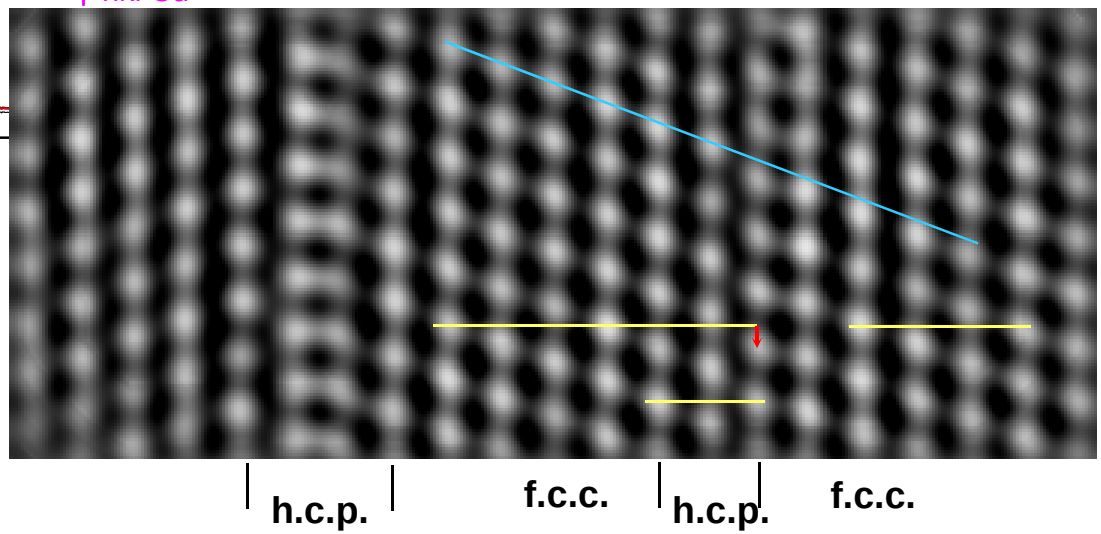

Summary

- Powder XRD can give information on crystalline phases identity (fingerprint), crystal structure and quantitative phase analysis (e.g. from Rietveld refinement) and size/strain effects (from line profile analysis)
- Neutron diffraction is a non-routine complementary technique allowing detection of light elements, recording of higher intensity Bragg reflections at high angle, discrimination of neighbouring elements, resolution of magnetic sub-lattices

References / Sources

- M. Behrens, R. Schlögl „X-Ray Diffraction and Small Angle X-Ray Scattering“ in Characterization of Solid Materials and Heterogeneous Catalysts: From Structure to Surface Reactivity, Edited by Michel Che and Jacques C. Vedrine, Wiley-VCH Weinheim 2011.
- L.H. Schwartz, J.B. Cohen “Diffraction from Materials” Academic Press, New York 1977.
- H.P. Klug, L.E. Alexander “X-Ray Diffraction Procedures” 2nd Edition, John Wiley, New York 1974.
- R.A. Yound (ed) “The Rietveld Method” IUCr, Oxford Science Publications, Oxford University Press 1993.
- S.E. Dann “Reaction and Characterization of Solids” RSC, Cambridge 2000.
- Educational material for the “Praktikum für Fortgeschrittene”, Institute of Inorganic Chemistry of the University Kiel.
- Helmhotz-Zentrum für Materialien und Energie: www.hmi.de.
- Handout “Weiterbildung Chemische Nanotechnologie”, Universität des Saarlands, Saarbrücken.
- Handout “Application of Neutrons and Synchroton Radiation in Engineering Material Science”, Virtual Institute Photon and Neutrons for Advanced Materials (PNAM).
- J. I. Langford, A. Boultif, J. P. Auffrédic, D. Louër, *J. Appl. Crystallogr.* 1993, 26, 22.
- F. Girgsdies: Lecture Series Modern Methods in Heterogeneous Catalysis: “X-Ray Diffraction in Catalysis” 2006.